NIH Public Access
Author Manuscript
J Immunol. Author manuscript; available in PMC 2015 January 01.

Published in final edited form as:
J Immunol. 2014 January 1; 192(1): . doi:10.4049/jimmunol.1302586.

Calcium signaling via Orai1 is essential for induction of nuclear orphan receptor pathway to drive T_H17 differentiation

Kyun-Do Kim[#1], **Sonal Srikanth**[#1], **Yossan-Var Tan**[2], **Ma-Khin Yee**[1], **Marcus Jew**[1], **Robert Damoiseaux**[3], **Michael E. Jung**[4], **Saki Shimizu**[5,6], **Dong Sung An**[5,6,7], **Bernard Ribalet**[1], **James A. Waschek**[2], and **Yousang Gwack**[1]

[1]Department of Physiology, David Geffen School of Medicine at UCLA, Los Angeles, CA 90095, USA

[2]The NPI-Semel Institute and Department of Psychiatry, David Geffen School of Medicine at UCLA, Los Angeles, CA 90024, USA

[3]Molecular Screening Shared Resources, UC CEIN, NanoSystems Institute, University of California, Los Angeles, CA90095, USA

[4]Department of Chemistry and Biochemistry, University of California, Los Angeles, CA90095, USA

[5]Division of Hematology-Oncology, David Geffen School of Medicine at UCLA

[6]UCLA AIDS Institute, Los Angeles, CA 90095, USA

[7]UCLA School of Nursing, Los Angeles, CA 90095, USA

[#] These authors contributed equally to this work.

Abstract

Orai1 is the pore subunit of Ca^{2+} release-activated Ca^{2+} (CRAC) channels that stimulate downstream signaling pathways crucial for T cell activation. CRAC channels are an attractive therapeutic target for alleviation of autoimmune diseases. Using high throughput chemical library screening targeting Orai1, we identified a novel class of small molecules that inhibit CRAC channel activity. One of these molecules, compound 5D inhibited CRAC channel activity by blocking ion permeation. When included during differentiation, T_H17 cells showed higher sensitivity to compound 5D than T_H1 and T_H2 cells. The selectivity was attributable to high dependence of promoters of retinoic-acid-receptor-related orphan receptors on Ca^{2+}-nuclear-factor-of-activated-T cells (NFAT) pathway. Blocking of CRAC channels drastically decreased recruitment of NFAT and histone modifications within key gene loci involved in T_H17 differentiation. The impairment in T_H17 differentiation by treatment with CRAC channel blocker was recapitulated in Orai1-deficient T cells, which could be rescued by exogenous expression of retinoic-acid-receptor-related orphan receptors or a constitutive active mutant of NFAT. In vivo administration of CRAC channel blockers effectively reduced the severity of experimental

Address correspondence and reprint requests to Yousang Gwack, Department of Physiology, David Geffen School of Medicine at UCLA, 53-266 CHS, 10833 Le Conte Avenue, Los Angeles, CA 90095. ygwack@mednet.ucla.edu.

Author Contributions

S.S. and Y.G. designed the research; S.S. performed chemical library screens and human PBMC experiments with technical help from M.K.Y., M.J., and R.D.; S.S. and B.R. performed and analyzed patch clamp experiments; K.D.K. analyzed T cell phenotypes and performed EAE experiments with Y.V.T under the guidance of J.A.W.; M.E.J. contributed to chemical designing; A.D.S and S.Shimizu assisted in human PBMC experiments; S.S., K.D.K., and Y.G. wrote the manuscript and Y.G supervised the project.

Disclosures

The authors declare no competing financial interests.

NIH-PA Author Manuscript
NIH-PA Author Manuscript
NIH-PA Author Manuscript

NIH-PA Author Manuscript

NIH-PA Author Manuscript

NIH-PA Author Manuscript

autoimmune encephalomyelitis by suppression of differentiation of inflammatory T cells. These results suggest that CRAC channel blockers can be considered as chemical templates for development of therapeutic agents to suppress inflammatory responses.

Introduction

Stimulation of T cell receptor (TCR) evokes Ca^{2+} entry via CRAC channels (1). An increase in intracellular Ca^{2+} concentration ($[Ca^{2+}]_i$) induces proliferation and cytokine production in immune cells by activation of downstream target molecules including NFAT (2). The Ca^{2+}-bound calmodulin/calcineurin protein phosphatase complex dephosphorylates heavily phosphorylated, cytoplasmic NFAT, which in turn translocates into the nucleus and turns on various transcriptional programs. Orai1 was identified as the pore component of CRAC channels by genome-wide RNAi high throughput screens (3-6). Human patients with a homozygous missense mutation in *ORAI1* suffer from lethal, severe combined immunodeficiency (SCID) (5). Earlier, stromal interaction molecule 1 (STIM1) was identified as an important signaling molecule in the CRAC channel pathway using limited RNAi screens (7, 8). TCR stimulation induces phospholipase (PLC) γ-mediated depletion of endoplasmic reticulum (ER) Ca^{2+} stores. STIM1 senses ER Ca^{2+} depletion via its EF hands and translocates into the ER-plasma membrane (PM) junctions to activate Orai1, thereby causing a sustained increase in $[Ca^{2+}]_i$ (7, 9, 10). This sequential activation mechanism was termed as store-operated Ca^{2+} entry (SOCE) since depletion of ER Ca^{2+} stores precedes CRAC channel activation (11). Patients with homozygous nonsense mutation in *STIM1* also suffered from SCID, further emphasizing the crucial role of CRAC channels in the immune system (12). Recently several reports have described the immune phenotypes of Orai1- and STIM1-deficient mice. These mice showed a defect in immune cells, consistent with the SCID patients (13-17).

Upon stimulation, naïve $CD4^+$ T cells differentiate into distinct effector cell types including T_H1, T_H2, and T_H17 cells. Accumulating data suggest that T_H17 cells are highly pro-inflammatory and essential for severe autoimmunity in various disease models including a murine model of multiple sclerosis, experimental autoimmune encephalomyelitis (EAE). During differentiation of T_H17 cells, cytokines including IL-1, IL-6, IL-21, IL-23, and TGF-β promote IL-17 production and expression of lineage-specific transcription factors including retinoic-acid-receptor-related-orphan-receptor (ROR)γt and RORα (18-23). Individual or combined deletion of RORγt and RORα drastically reduced T_H17 cell differentiation and accordingly, these mice showed a strong resistance to EAE (24).

In T_H1-T_H2 paradigm, it is well known that TCR signaling contributes to the differentiation of naïve T cells into lineage-specific effector T cells. Previous studies have shown that the strength of TCR stimulation plays an important role in lineage specification, with stronger stimulation favoring differentiation into T_H1 cells and weaker stimulation favoring T_H2 differentiation (25). In the case of T_H17 cells, it is known that TCR stimulation in conjunction with cytokines is crucial for differentiation (21-23). However, the contribution of TCR stimulation-induced Ca^{2+} signaling pathway underlining T_H17 differentiation remains poorly understood, partly due to the recent identification of Orai1 and STIM1.

Using genome-wide RNAi screens in *Drosophila* cells that utilized NFAT-GFP translocation to the nucleus as readout, we identified two novel families as regulators of NFAT, dual-specificity tyrosine-regulated kinases (DYRKs) and Orai Ca^{2+} channels (5, 6, 26). Here, we extended a similar strategy to chemical library screens using a mammalian cell-line exhibiting amplified CRAC channel activity. High throughput screening from a total of ~85,000 chemicals lead to identification of a novel class of small molecule

NIH-PA Author Manuscript

NIH-PA Author Manuscript

NIH-PA Author Manuscript

compounds as CRAC channel inhibitors. Treatment with these compounds strongly blocked differentiation of T_H17 cells in vitro and in vivo with higher sensitivity when compared to T_H1 and T_H2 cells. At a molecular level, treatment with one of the blockers, compound 5D, reduced expression levels of RORα and RORγt transcription factors during T_H17 differentiation, and this defect was rescued by overexpression of RORα, RORγt, and a constitutively active mutant of NFAT. Furthermore, treatment with compound 5D strongly reduced active chromatin marks of RORα, RORγt and IL-17 promoters. These results reveal a direct role of Orai-NFAT pathway in regulation of RORα and RORγt expression during T_H17 differentiation. Our study suggests that derivatives of compound 5D can be used as chemical templates for development of therapeutic agents to alleviate inflammation and as molecular probes to investigate the role of TCR stimulation-mediated Ca^{2+} entry in inflammatory diseases.

Materials and Methods

Reagents and antibodies

Thapsigargin and 2-APB were purchased from EMD Chemicals (Billerica, MA). Following antibodies were obtained from eBioscience (San Diego, CA) and utilized for surface and intracellular staining – CD4 (GK1.5), IL-4 (11B11), IFN-γ (XMG1.2), IL-17A (eBio17B7) and RORγt (AFKJS-9).

Plasmids

Full-length cDNA of human Orai1 was subcloned into bicistronic retroviral expression vector pMSCV-CITE-eGFP-PGK-Puro (which allows for simultaneous expression of Orai1, GFP and a puromycin resistance gene) and has been described previously (27). Single-point mutants were generated using Quickchange XL site-directed mutagenesis kit (Stratagene, Santa Clara, CA) following manufacturer's instructions. All the clones were verified by sequencing. For total internal reflection fluorescence (TIRF) analysis, WT Orai1 cDNA was fused in frame with pEGFP to have a C-terminal GFP-tag. STIM1-mCherry plasmid has been described previously (27, 28). Orai1 $Q^{108}LD^{110} \rightarrow A^{108}AA^{110}$ and $D^{110}AD^{112}>A^{110}AA^{112}$ were generated by introducing a NotI site in the primers. Orai1 ΔEC2 clone was generated by deletion of amino acids L^{202}-P^{231} within the second extracellular loop by introduction of a NotI restriction enzyme site.

Cell-lines and transductions

HEK293 cells were obtained from ATCC and cultured in Dulbecco's modified Eagle's medium (DMEM - Mediatech, Hargrave, VA) supplemented with with 10% fetal bovine serum (Hyclone, Logan, UT), 10 mM HEPES, 10 mM Glutamine and 1% penicillin/ streptomycin (Mediatech, Hargrave, VA). Cells were transfected at 60-70% confluency using Lipofectamine 2000 (Invitrogen, Carlsbad, CA) according to the manufacturer's instructions. For retroviral transductions, phoenix cells stably expressing gag-pol and ecotropic env (purchased from ATCC) were transfected with plasmids encoding Orai cDNAs to produce ecotropic, replication-incompetent retrovirus using calcium phosphate transfection method. Virus-containing supernatant was collected at 2 and 3 days after transfection and immortalized $Orai1^{-/-}$ murine embryonic fibroblasts (MEFs) (13) or primary T cells were transduced in the presence of 8 μg/ml polybrene. Transduction efficiencies were evaluated visually by GFP expression.

High throughput screen to identify small molecule blockers of CRAC channels

HeLa cells stably expressing Orai1, STIM1 and NFATc2-1-460-GFP (NFAT-GFP) were generated by retroviral transduction with viruses encoding each cDNA and antibiotic

NIH-PA Author Manuscript

NIH-PA Author Manuscript

NIH-PA Author Manuscript

selection. Cells were FACS-sorted for selection of GFP^{high} population. ~5000 cells were plated onto individual 384-well plates coated with poly-L-Lysine (Greiner Bio-one, Monroe, NC). Next day, the cells were washed twice with 2 mM Ca^{2+}-containing Ringer solution and bathed in the same solution. Compounds were added using a 384-well pin tool (V&P Scientific, Inc., San Diego, CA) at a final concentration of 10 μM. Cells were incubated with the compounds for 5 mins and then treated with a final concentration of 1 μM thapsigargin for ~30 mins, fixed, permeabilized and stained with 4′,6-diamidino-2-phenylindole (DAPI), and the coincident GFP and DAPI images were acquired by an automated camera from each well. Every plate included two type of controls; one without any compound to monitor nuclear translocation of NFAT-GFP and another with 100 μM 2-APB to visualize block of NFAT-GFP nuclear translocation. Only the plates showing expected patterns for control wells were used for further evaluation. The chemical libraries of Biomol, FDA-approved drugs, MicroSource, Prestwick, Chembridge, Druggable compounds and lead-like compounds totaling to ~85,000 small molecule compounds were used in the primary screen. Candidates from the primary screen were cherry-picked into 96-well plates and a confirmatory screen was performed in triplicates using the protocol described above. Positive candidates from the confirmatory screen were then examined for their blocking efficacy on SOCE using single-cell Ca^{2+} imaging.

Single-cell Ca^{2+} imaging

HeLa O+S cells and fibroblasts were grown directly on UV-sterilized coverslips and loaded with 2 μM Fura 2-AM for 45 min. Primary T cells were loaded with 1 μM Fura 2-AM for 30 min and attached onto poly-D-Lysine coated coverslips. For $[Ca^{2+}]_i$ measurements, cells were mounted on a RC-20 closed bath flow chamber (Warner Instrument Corp., Hamden, CT) and analyzed on an Olympus IX51 epifluorescence microscope with Slidebook (Intelligent Imaging Innovations, Inc.) imaging software. Cells were perfused with Ca^{2+}-free Ringer's solution, and Ca^{2+} stores were passively depleted with 1 μM of thapsigargin. Store-operated Ca^{2+} entry (SOCE) was measured by exchanging the Ca^{2+}-free Ringer's solution with that containing 2 mM $CaCl_2$. At the peak of SOCE, cells were exposed to the same solution containing 10 μM (or different concentrations) of individual blockers. Fura-2 emission was detected at 510 nm with excitation at 340 and 380 nm, and the Fura-2 emission ratio (340/380) was acquired at every 5-s interval after background subtraction. For each experiment, 50–100 individual cells were analyzed using OriginPro (Originlab, Northampton, MA) analysis software. Peak-basal Ca^{2+} ratio was calculated after subtracting the ratio value after store depletion, before reintroduction of Ca^{2+} containing Ringer's solution from the maximal value of 340/380 ratio after reintroduction of Ca^{2+} containing Ringer's solution. Sustained Ca^{2+} was calculated as the 340/380 ratio at the time point of 800s after subtracting basal Ca^{2+} ratio.

Total internal reflection fluorescence microscopy (TIRFM) analysis

HEK293 cells were transfected with plasmids encoding STIM1-mCherry along with WT Orai1-GFP fusion protein encoding cDNAs at a molar ratio of 1:1. TIRFM was performed using an Olympus IX2 illumination system mounted on an Olympus IX51 inverted microscope. Laser beams from a 488 nm argon ion laser (Melles Griot, Carlsbad, CA) and a 594 nm diode laser (Cobolt instruments, San Jose, CA) were combined and controlled using an Olympus OMAC TIRF dual port condenser and controller system. The angle of the incident light at the interface between the glass coverslip and the aqueous medium was controlled by independently adjusting the position of each laser beam before passing through a 60x oil-immersion objective (NA 1.49, Olympus). The emission was filtered either at D525/50 or 660/50 nm filter (Chroma Technology Corp., Bellows Falls, VT) and captured by a Hamamatsu ORCA cooled CCD (Roper Scientific, Tucson, AZ) camera.

NIH-PA Author Manuscript

NIH-PA Author Manuscript

NIH-PA Author Manuscript

Acquisition and image analysis were performed using Slidebook (Intelligent Imaging Innovations, Inc., Denver, CO) and OriginPro8.5 software.

Measurement of CRAC currents by whole-cell recording

For recording of CRAC currents, HEK293 cells were co-transfected with plasmids encoding Orai1 WT or mutant cDNAs in the presence or absence of STIM1 encoding plasmid at a molar ratio of 1:1 using Lipofectamine 2000 (Invitrogen, Carlsbad, CA). Cells were used for experiments 24-48 hrs post transfection. Patch-clamp recordings were performed using an Axopatch 200B amplifier (Molecular Devices, California) interfaced to a Digidata 1320A (Axon Instruments, CA) for stimulation and data acquisition. Currents were filtered at 1 kHz with a 4-pole Bessel filter and sampled at 5 kHz. Recording electrodes were pulled from borosilicate glass capillaries (WPI, Sarasota, Fl) using a Flaming Brown pipette puller (Sutter Instrument, CA) to a final resistance of 2-7 MΩ. Stimulation, data acquisition, and analysis were performed using pCLAMP8 and Origin software. The standard extracellular Ringer solution contained (in mM): 145 Cs–aspartate, 4.5 KCl, 6 $CaCl_2$, 10 D-glucose, and 10 Na-Hepes (pH 7.35). The standard internal solution contained (in mM): 145 Cs-glutamate, 8 $MgCl_2$, 12 EGTA, and 10 Cs-Hepes (pH 7.3). Unless otherwise stated the cell membrane was held at 0 mV and pulses were applied between −110 mV to +115 mV at 15 mV intervals for 250 ms.

Analysis of patch clamp data.

Ionic currents from cells expressing WT and mutant channels were recorded using only the analog compensation of the membrane linear components. In some cases (mutant channels) the blocker(s) had no inhibitory effects and the current traces could not be corrected for leak currents. The first 1 ms of recorded data following the onset of the voltage pulses, was not included in the fitting to minimize the effect of uncompensated membrane capacitance on the estimated time course of the current. For the I-V, steady state currents measured at the end of the pulse were used.

T cell isolation and differentiation

$CD4^+$ T cells were purified from single-cell strained suspensions prepared by mechanical disruption of spleens and lymph nodes of adult mice after magnetic sorting with $CD4^+$ beads (Invitrogen). $CD4^+CD25^-$ naïve T cells were selected by CD25 MACS positive selection (Miltenyi Biotec, Auburn, CA). For effector T cell differentiation, cells were stimulated with 2 μg/ml of anti-CD3 (Bio X cell, West Lebanon, NH) and anti-CD28 (Bio X cell, West Lebanon, NH) antibodies for 48 hours on a plate coated with 0.1 mg/ml of goat anti-hamster (MP Biomedicals, Solon, OH). $CD4^+CD25^-$ T cells were cultured with 10 μg/ml anti-IL-4 (Bio X cell), and 10 ng/ml IL-12 for T_H1 differentiation, 20 μg/ml anti-IFN-γ (Bio X cell, West Lebanon, NH), 2.5 μg/ml anti-IL-12 and 10 ng/ml IL-4 (Peprotech, Rocky Hill, NJ) for T_H2 differentiation, and 10 μg/ml anti-IL-4, 20 μg/ml anti-IFN-γ, 30 ng/ml IL-6 (Peprotech, Rocky Hill, NJ), 3 ng/ml TGF-β (Peprotech, Rocky Hill, NJ) and 10 ng/ml IL-23 (R&D Systems, Minneapolis, MN) for T_H17 differentiation. On day 4, differentiated T cells were restimulated with 20 nM phorbol myristate acetate (PMA) and 1 μM ionomycin for cytokine analysis.

Active EAE induction in mice

All animals were maintained in pathogen-free barrier facilities and used in accordance with protocols approved by the Institutional Animal Care and Use Committee at the University of California, Los Angeles. For induction of EAE, mice were immunized subcutaneously on day 0 with 100 μg of $MOG_{35–55}$ peptide (N-MEVGWYRSPFSRVVHLYRNGK-C, Genscript) emulsified in complete Freund's adjuvant (CFA, Difco, Houston, TX)

NIH-PA Author Manuscript

NIH-PA Author Manuscript

NIH-PA Author Manuscript

supplemented with 5 mg/mL of Mycobacterium tuberculosis H37Ra (Difco, Houston, TX). These mice were also injected i.p. with 200 ng/mouse of pertussis toxin (List Biological Laboratories, Campbell, CA) on day 0 and 2. EAE was scored according to the following clinical scoring system: 0, no clinical signs; 1, limp tail; 2, partial hind leg paralysis; 3, complete hind leg paralysis or partial hind and front leg paralysis; 4, complete hind and partial front leg paralysis. Mice were injected i.p. with either the vehicle (DMSO, 50 μl), compound 5D (1 mg/kg) or 5J-4 (2 mg/kg) every alternate day starting from day 0.

T cell analysis

Draining lymph nodes were collected 14 days after EAE induction, and cell suspensions were prepared. For proliferation analysis, cells were distributed in a 96-well plate at 1×10^6 cells/ml concentration and cultured in media. Cell suspensions were restimulated with 20 μg/ml of MOG_{35-55} for 2 days at 37°C with 5% CO_2 and humidified atmosphere. All the cultures were run in triplicates. After 48 h, cultures were pulsed with 1 μCi/well [^{3}H]-thymidine (Amersham Biosciences, Piscataway, NJ) for an additional 16–18 h. After this treatment, cells were harvested, lysed, and acid precipitated. Finally, [^{3}H]-thymidine incorporation was determined by liquid β-scintillation counting (Beckman Coulter, Brea, CA). For intracellular staining, cells were distributed in a 12-well plate at 1×10^6 cells/ml concentration and cultured with 20 nM PMA and 1 μM ionomycin for 5h. For Real-time PCR, the total RNA of draining lymph nodes was extracted with TRIzol reagent (Invitrogen, Carlsbad, CA) following the manufacturer's instructions. For ex vivo experiments, draining lymph nodes were collected 7 days after EAE induction, and cell suspensions were prepared. Cells were distributed in a 12-well plate at 1×10^6 cells/ml concentration and cultured for four more days with the MOG peptide (20 μg/ml) together with exogenous IL-6 and IL-23 or IL-12, in the presence or absence of compound 5D.

Isolation of mononuclear cells from the central nervous system

To isolate mononuclear cells from phosphate-buffered saline (PBS)-perfused spinal cords and brain, tissues were digested in collagenase and DNase I (Roche) for 30 min at 37°C, and cells were separated on a 40-80% Percoll gradient by centrifugation at 500g for 30 min. Cells at the 40-80% interface were collected. For intracellular cytokine staining, cells were stimulated with 20 nM PMA and 1 μM ionomycin in the presence of 3 μg/ml brefeldin A (eBioscience, San Diego, CA) for 5 h and stained for CD4, IFN-γ, and IL-17A.

Histology

Following perfusion with PBS, spinal cords were removed and fixed with 4% paraformaldehyde in PBS at 4°C overnight. Tissues were blocked in paraffin wax. Sections (5 μm) were cut from paraffin block. Paraffin-embedded sections were stained with H&E and Luxol Fast Blue for visualization of inflammatory infiltrates and demyelination.

Real-time quantitative PCR

cDNA was synthesized from total RNA using oligo(dT) primers and Superscript III First-Strand cDNA synthesis kit (Invitrogen). Real-time PCR was performed using an iCycler IQ5 system (Biorad) and SYBR Green dye (Sigma) using the primers described in Supplementary Table 1. Threshold cycles (C_T) for all the candidate genes were normalized to the C_T values for beta-actin housekeeping gene control to obtain ΔC_T. The specificity of primers was examined by melt-curve analysis and agarose gel electrophoresis of PCR products.

NIH-PA Author Manuscript

NIH-PA Author Manuscript

NIH-PA Author Manuscript

Chromatin immunoprecipitation (ChIP)

After culturing naïve T cells under T_H17-polarizing conditions with plate-coated anti-CD3 and anti-CD28 antibodies for 16 hours, cells were fixed for 8 min at room temperature with 1:37 dilution of 37.1 % formaldehyde (Calbiochem), neutralized with 1:20 dilution of 2.5 M glycine and washed twice in ice-cold phosphate buffered saline. Cells were lysed in 500 μl of low salt buffer (0.1% SDS, 1% Triton X-100, 2 mM EDTA, 20 mM Tris-HCl, PH 8.1, 150 mM NaCl), and chromatin sheared by sonication to generate 200-800 bp DNA fragments. For immunoprecipitation with anti-acetyl-Histone H3-K14 (Cat. #07-353; Millipore), anti-acetyl-Histone H3-K9 (Cat. #07-352; Millipore), and anti-NFAT1 antibody (clone 67.1), chromatin from $1x10^7$ whole-cell equivalents was used. Chromatin was diluted in low salt washing buffer and immunoprecipitation was performed by overnight incubation with the indicated antibodies, followed by 2 hours (at 4°C) incubation with 3 μg of Protein A sepharose CL-4B (GE Healthcare). Immunocomplexes were captured and washed twice for 5 min each with low salt washing buffer, high salt washing buffer (0.1% SDS, 1% Triton X-100, 2 mM EDTA, 20 mM Tris-HCl, PH 8.1, 500 mM NaCl), LiCl washing buffer (0.25 M LiCl, 1% NP-40, 0.1% deoxycholate, 1 mM EDTA, 10 mM Tris 8.1), and TE buffer (Tris-HCl 10 mM, EDTA 1 mM). Beads were resuspended in TE and then treated with 5 μl of 1 mg/ml RNase A for 30 mins at 37°C, and, finally, with proteinase K (0.2 mg/ml, Roche) overnight at 37°C. The samples were heated to reverse crosslinking at 65°C overnight. DNA was purified using Phenol–chloroform extraction and ethanol precipitation. Selected DNA sequences were quantified by real-time quantitative PCR using primers described in Supplementary Table 1. ChIP data are presented as the percentage recovery of input.

Human PBMC culture

Mononuclear cells were prepared from buffy coats from healthy, unidentified adult donors, obtained under federal and state regulations from the University of California, Los Angeles (UCLA) CFAR Gene and Cellular Therapy Core Laboratory. PBMCs were activated with anti-CD3/CD28 beads (Miltenyi Biotech) and cultured in T cell media (DMEM containing 20% Fetal bovine serum and 1% Pen-Strep) supplemented with 20 U/ml IL-2 (Peprotech), 10 ng/ml IL-1β, and 10 ng/ml IL-23 (eBioscience) in the presence or absence of 20 μM of compound 5D. Cells were expanded with fresh media, cytokines and compound 5D every alternate day. On day 6, cells were extensively washed and activated with 20 nM of PMA, 1 μM of ionomycin, and Brefeldin A (3 μg/ml) for 5 hrs, surface stained with anti-CD4-FITC, and intracellularly stained with anti-IL-17A-APC and anti-IFN-γ-PE. CD4-FITC-positive cells were gated for analysis. For flow cytometry, the following human specific antibodies were used: CD4-FITC (OKT4, eBioscience), IL-17A-APC (eBio64CAP17, eBioscience) and IFN-γ-PECy7 (45.B3, eBioscience).

Statistical analysis

Statistical analysis was carried out using two-tailed Student's t-test. Differences were considered significant when p values were <0.05.

Results

Identification of a small molecule blocker of Orai1, compound 5 from a chemical library screen

To develop a high throughput screen to identify Orai1 inhibitors, we generated a cell-line in which the CRAC currents (I_{CRAC}) are amplified by stable expression of Orai1 and STIM1 (27). A pilot screen using direct measurement of cytoplasmic Ca^{2+} concentration ($[Ca^{2+}]_i$) provided a Z′ factor of ~0.5. Earlier, using NFAT translocation as readout for CRAC

NIH-PA Author Manuscript

NIH-PA Author Manuscript

NIH-PA Author Manuscript

channel activity in *Drosophila* cells, we specifically selected ~20 candidates from a genome-scale RNAi screen (5, 6). Therefore, we generated HeLa-O+S cells stably expressing NFATc2 (amino acid 1-460)-GFP (abbreviated NFATGFP) to utilize nuclear translocation of NFAT-GFP as readout (Fig. 1A). Nuclear translocation of NFAT in HeLa-O+S cells triggered by store depletion was specifically suppressed by blocking CRAC channels with 2-APB suggesting that it is predominantly regulated by CRAC channel activity. A pilot screen utilizing NFAT translocation as readout showed a Z′ factor of ~0.7, providing an ideal platform for high throughput screening. A chemical library encompassing ~85,000 compounds was screened to identify blockers of NFAT translocation. Each plate included a positive control, 2-APB and plates were automatically scored for colocalization of NFAT-GFP and 4,6-diamidino-2-phenylindole (DAPI) signals. Candidates affecting survival or morphology of the cells were excluded from further analyses. Positive candidates from the primary screen were further examined for direct block of SOCE using single cell ratiometric Ca^{2+} imaging. This analysis resulted in identification of compound 5, N-[2,2,2-trichloro-1-(1-naphthylamino)ethyl]-2-thiophenecarboxamide as a specific inhibitor of CRAC channels (Fig. 1B).

A structural analogue of compound 5 potently blocks CRAC channel activity

To identify compounds with better blocking efficacy, structural analogues of compound 5 were examined for block of SOCE in HeLa-O+S cells. Among these, compound 5D, N-[2,2,2-trichloro-1-(2-naphthylamino)ethyl]-2-furamide showed an enhanced block of SOCE (Fig. 1B and Suppl. Fig. 1A). Modifications in the structure of the thiophene or naphthalene rings of compound 5 reduced the blocking effect suggesting their important role in inhibiting CRAC channel activity (data not shown). We next examined the blocking efficacy of compound 5D on endogenous CRAC channels in primary $CD4^+$ T cells. Compound 5D blocked endogenous SOCE, especially sustained Ca^{2+} levels of effector T cells in a dose-dependent manner with a half-maximum inhibitory concentration (IC_{50}) of 807 nM and 195 nM for the peak and sustained levels of SOCE, respectively (Fig. 1C).

Compound 5D inhibits CRAC channel activity by blocking ion permeation

The CRAC channel has unique gating and inactivation mechanisms. ER store depletion induces multimerization and clustering of STIM1 at the ER-PM junctions, which allows for a direct protein interaction between Orai1 and STIM1 (1). To elucidate the molecular mechanism of inhibition by compound 5D, we measured the effect of compound 5D at different stages of Orai1 activation. First, we examined whether presence of compound 5D altered accumulation of STIM1 and Orai1 at the ERPM junctions using total internal reflection fluorescence (TIRF) microscopy. These studies showed no significant effect of compound 5D on the rate or extent of accumulation of Orai1 or STIM1 at the ERPM junctions (Suppl. Fig. 1B). Next, to examine the effect of compound 5D on CRAC currents, we used HEK293 cells transiently expressing Orai1 and STIM1. In these cells, we could detect large I_{CRAC} that was almost completely blocked by compound 5D when applied in the external solution, while intracellular application via the patch pipette had no effect (Fig. 1D). These results suggested that the binding site of compound 5D is located at or near the extracellular region of Orai1.

Orai1 contains four transmembrane segments (TM1-4), cytoplasmic N and C termini, and two extracellular loops EC1 and EC2 with TM1 lining the pore (Fig. 1E). Recently, we showed that the mutation W176C in TM3 resulted in STIM1-independent, constitutively active CRAC currents (29). Compound 5D could reversibly inhibit currents generated from $Orai1^{W176C}$ (Fig. 1F and Suppl. Fig. 1C), suggesting that blocking by compound 5D is independent of STIM1 interaction with Orai1. Previous mutational analysis of transmembrane segments of Orai1 suggested that residues L95, G98 and V102 in TM1

NIH-PA Author Manuscript

NIH-PA Author Manuscript

NIH-PA Author Manuscript

segment of Orai1 are directly involved in ion permeation (30, 31). Since Orai1 inhibitor compound 5D blocks CRAC currents when applied extracellularly, we mutated conserved residues in the two EC loops as well as in TM1 that can be accessible from the extracellular milieu when the channel is open. Various mutants of Orai1 in TM1 and two EC loops were expressed in Orai1$^{-/-}$ murine embryonic fibroblasts (MEFs) and examined for block of SOCE (Fig. 1F). It has been suggested that extracellular loop 1, which contains three aspartate residues (D^{110}×D^{112}×D^{114}), forms the channel's outer vestibule and is possibly involved in ion selectivity (1). Mutation of these residues (mutants $Q^{108}LD^{110}$>AAA and $D^{110}AD^{112}$>AAA) did not affect blocking by compound 5D. In addition, deletion of extracellular loop 2 (ΔEC2) also did not affect block by compound 5D. Recent studies suggested that residue V102 within TM1 may form the gate that opens and closes CRAC channels and its mutation results in STIM1-independent and constitutively active channels (32). Our mutational analysis of this residue demonstrated a very slow and partial block of Orai1^{V102C} and Orai1^{V102A}-evoked currents by compound 5D (Fig. 1F, Suppl. Fig. 1D and E). These data suggest that compound 5D specifically blocks Orai family of channels by binding at or near V102 (of Orai1) to close the channel although we cannot rule out the possibility of its binding to a remote site and allosterically causing closure of the channel gate at V102.

Compound 5D did not have any effect on Ca^{2+} entry mediated by TrpC1 (transient receptor potential canonical) channels, a member of TrpC family of store-operated Ca^{2+} channels, when co-expressed with STIM1 in HEK293T cells (Suppl. Fig. 1F). To examine if compound 5D blocked SOCE via other Orai proteins, we transduced Orai1-deficient T cells with retroviruses for expression of Orai2 and Orai3 proteins (13). We observed block of residual SOCE in Orai1-deficient T cells, which is likely to be mediated by Orai2 or Orai3 proteins (Suppl. Fig. 1G) (13, 33). Expression of all the Orai proteins enhanced SOCE in Orai1-deficient T cells, supporting earlier observation that all three Orai proteins can be activated by store depletion (34, 35). Importantly, compound 5D treatment blocked SOCE mediated by all three Orai proteins (Suppl. Fig. 1G). Collectively, our results suggests that compound 5D specifically blocks Orai proteins by binding to a site facing the extracellular milieu and its inhibitory mechanism involves the potential channel gate located at V102.

T_H1, T_H2, and T_H17 differentiation exhibit different sensitivity to CRAC channel inhibition

To analyze the effect of compound 5D on SOCE in various T cells, we measured SOCE from naïve and stimulated murine T cells cultured under T_H1, T_H2, and T_H17-polarizing conditions. While compound 5D blocked SOCE in T_H1, T_H2, as well as T_H17 cells, the block was stronger for differentiated T_H17 cells when compared with that of naïve, T_H1 or T_H2 cells (Fig. 2A). Consistent with these results, IL-17A production by T_H17 cells was more severely affected when compared to IFN-γ and IL-4 production by T_H1 and T_H2 cells respectively, in the presence of compound 5D (Fig. 2B and C). Next, to determine the effect of inhibition of SOCE on T cell differentiation, we stimulated naïve T cells under T_H1, T_H2, and T_H17-polarizing conditions in the presence and absence of compound 5D. In these experiments, compound 5D was included specifically during the differentiation stage but excluded during restimulation to examine cytokine production. Presence of compound 5D during differentiation blocked cytokine production by T_H1, T_H2, as well as T_H17 cells; however, T_H17 cells showed a stronger block of IL-17A production when compared to IFN-γ and IL-4 production by T_H1 and T_H2 cells respectively (Fig. 2D). Analysis of lineage-specific cytokines and transcription factors showed a pronounced reduction of mRNA levels of IL-17A, RORα and RORγt under T_H17-polarized conditions even with low concentrations of compound 5D, compared to those of IFN-γ and T-bet under T_H1-polarized conditions, or IL-4 and GATA-3 under T_H2-polarized conditions (Fig. 2E). Contrary to T_H17 cells, differentiation of regulatory T cells (iTregs) was not significantly influenced by

NIH-PA Author Manuscript

NIH-PA Author Manuscript

NIH-PA Author Manuscript

treatment with compound 5D as judged by expression levels of Foxp3 (Suppl. Fig. 2A). Previous studies have shown that T_H17 cells have a distinct Ca^{2+} profile when compared to T_H1 and T_H2 cells (36). Since T_H17 cells showed higher sensitivity to block by compound 5D and the role of SOCE and NFAT family of transcription factors in differentiation of T_H17 cells is less understood, we focused our studies on T_H17 cells. We observed reduced expression levels of molecules involved in T_H17 pathogenicity including IL-23 receptor (IL-23R), CCR6, and integrin αL (LFA-1) in compound 5D-treated cells (Suppl. Fig. 2B). While inhibition of factors including c-Maf, Runt-related transcription factor 1 (Runx1), aryl hydrocarbon receptor (AHR), interferon-regulatory factor 4 (IRF-4), suppressor of cytokine signaling 3 (SOCS3), IκBζ, basic leucine zipper transcription factor ATP-like (BATF), or hypoxia-inducible factor 1 (HIF1), all of which are known to play an important role in T_H17 differentiation (Suppl. Fig. 2C) (38-44). These data suggest a selective role of Orai1-mediated Ca^{2+} signaling in regulating the expression levels of RORα and RORγt during T_H17 differentiation.

Next, we investigated if compound 5D inhibits in vitro expansion/maintenance of antigen-specific effector T cells. For these experiments, wild-type mice were injected with a peptide derived from myelin oligodendrocyte glycoprotein (MOG_{35-55} peptide) emulsified with complete Freund's adjuvant (CFA) and after 7 days, draining lymph nodes were harvested. Cells from the draining lymph nodes were cultured with MOG_{35-55} peptide plus exogenous IL-12 or IL-23 with or without compound 5D, and examined for IFN-γ- and IL-17A-producing populations. We observed reduction of both IFN-γ-and IL-17A in compound 5D-treated cells, however, the reduction of IL-17A-producing cells was more pronounced (Fig. 2F). These experiments suggested that in addition to de novo differentiation, expansion/ maintenance of pre-differentiated T_H17 cells also needed CRAC channel activity.

Expression of RORα and RORγt can reverse the inhibitory effect of compound 5D on T_H17 differentiation

So far, our data indicate that inhibition of Ca^{2+} signaling suppresses T_H17 differentiation and expansion. However, it is not clear whether this suppression is caused by indirect effect of blocking cell proliferation, inducing cell death, or inhibition of specific signaling pathways required for T_H17 differentiation. Thus, we examined IL-$17A^+$ populations during different division cycles of carboxyfluorescein succinimidyl ester (CFSE)-labeled cells incubated with compound 5D. Consistent with the important role of Ca^{2+} signaling in T cell proliferation after stimulation, treatment with compound 5D suppressed proliferation (Fig. 3A). However, even within the same division cycle, compound 5D-treated cells showed much lower IL-17 production. In addition, we did not observe any significant difference in cell death in the absence or presence of compound 5D under T_H17-polarizing conditions (data not shown). These results suggest that suppression of T_H17 differentiation by compound 5D is derived primarily from a direct block of signaling pathways, independent of cell proliferation or cell death.

Since treatment with compound 5D specifically reduced expression of RORα and RORγt in T_H17 cells, not other cellular factors (Fig. 2E, Suppl. Fig. 2C), we examined if overexpression of these transcription factors can override the inhibitory effect of compound 5D on T_H17 differentiation. Moderate expression of RORα or RORγt slightly enhanced IL-17A production in control cells; however, it significantly rescued IL-17A expression in compound 5D-treated cells (Fig. 3B). These results further demonstrated a direct role of CRAC channels in T_H17 differentiation by regulating the expression of RORα and RORγt.

NIH-PA Author Manuscript

NIH-PA Author Manuscript

NIH-PA Author Manuscript

Orai1-NFAT-RORα/γt axis plays a crucial role in T_H17 differentiation

Previous studies have predicted putative NFAT-binding elements within the RORγt promoter (45, 46). In addition, expression of a constitutively active NFATc2 mutant influenced expression of RORγt during early stages of T_H17 differentiation (47). Since NFAT family of transcription factors are directly activated by SOCE, we examined their role in regulating expression of RORα and RORγt. Naïve T cells were stimulated and cultured under T_H17-polarizing conditions in the presence of cyclosporine A (CsA), a calcineurin blocker that also inhibits nuclear translocation of NFAT. Blocking calcineurin activity during T_H17 differentiation severely reduced IL-$17A^+$ population, consistent with previous observations (Fig. 3C) (48). In addition, both mRNA levels of RORγt and RORα were reduced in the presence of CsA. These results suggested an important role for Ca^{2+}-NFAT signaling pathway in regulating RORα and RORγt expression. We next examined whether constitutive active NFAT (CANFAT) could rescue compound 5D treatment-induced defect in RORα and RORγt expression. As seen in Fig. 3D, exogenous expression of CA-NFAT in compound 5D-treated cells during differentiation resulted in a strong recovery of IL-$17A^+$ population as well as expression of RORα and RORγt.

To examine a direct role of NFAT in expression of RORα and RORγt, chromatin immunoprecipitation (ChIP) experiments were performed from naïve T cells stimulated and cultured under T_H17-polarizing conditions with and without compound 5D. These experiments demonstrated a direct recruitment of NFATc2, the predominant NFAT family member in naïve T cells (49), on the promoters of RORγt and RORα under T_H17-polarizing conditions, which was markedly reduced in compound 5D-treated cells (Fig. 4A, left two panels). We further examined the effect of compound 5D treatment on the chromatin structure of the RORγt and RORα promoters in naïve and T_H17-polarized $CD4^+$ T cells. We measured acetylation of histone-3 at lysine-9 or lysine-14 residues (H3K9/K14Ac), an indication of active transcription site and open chromatin structure, at the promoter regions of RORγt and RORα. These studies demonstrated a severe reduction in H3K9/14 acetylation at the promoter regions of RORγt and RORα in compound 5D-treated T cells (Fig. 4A, right two panels). Together, these results demonstrated an important role for Orai-Ca^{2+}-NFAT pathway in the transcription of RORγt and RORα, thereby T_H17 differentiation. Correspondingly, NFAT recruitment and acetylation of H3K9 and H3K14 at the conserved non-coding sequence (CNS) 2 and the promoter region of IL-17A were also dramatically reduced in compound 5D-treated cells cultured under T_H17-polarizing conditions (Fig. 4B). To examine the effect of blocking NFAT activity on T_H1 differentiation, we performed ChIP experiments from naïve T cells stimulated and cultured under T_H1-polarizing conditions. NFAT recruitment and histone acetylation at the promoter regions of T-bet and IFN-γ were less influenced by treatment with compound 5D (Fig. 4C). These results suggest that a higher sensitivity of T_H17 differentiation to compound 5D is at least partly caused by a strong dependence of promoters and enhancers of RORα, RORγt, and IL-17 on Ca^{2+}-NFAT signaling pathway.

Orai1-deficient T cells recapitulate defects in T_H17 differentiation observed in compound 5D-treated cells

To confirm whether compound 5D specifically blocked Orai1 activity, we examined T_H17 differentiation of $CD4^+$ T cells isolated from Orai1$^{-/-}$ mice (13). Similar to compound 5D-treated cells, Orai1$^{-/-}$ T cells cultured under T_H17-polarizing conditions showed drastically decreased expression levels of IL-17, RORα and RORγt (Fig. 5A and B). Transcript analysis showed a pronounced reduction in expression levels of cytokines and receptors including IL-17A, IL-17F, IL-22, and IL-23R in Orai1$^{-/-}$ T cells (Fig. 5C). To investigate if NFAT can recover the defective T_H17 differentiation observed in Orai1$^{-/-}$ T cells, we transduced these cells with CA-NFAT. Expression of CA-NFAT almost completely

NIH-PA Author Manuscript

NIH-PA Author Manuscript

NIH-PA Author Manuscript

recovered expression of RORα and RORγt and moderately rescued IL-17A expression in Orai1$^{-/-}$ cells (Fig. 5D). Furthermore, the recruitment of NFAT to the promoters of RORα and RORγt was severely decreased in Orai1$^{-/-}$ T cells cultured under T_H17-polarized conditions, similar to results obtained from compound 5D-treated cells (Fig. 5E). These results together with the rescue experiments from compound 5D-treated cells strongly suggested that expression of RORα and RORγt is regulated by Orai-Ca^{2+}-NFAT signaling pathway.

Amelioration of EAE by CRAC channel inhibition

To examine the effects of CRAC channel inhibition in vivo, we utilized a mouse model of inflammation, EAE, where the pathogenic function of inflammatory T cells is extensively studied. Compound 5D treatment greatly ameliorated EAE in vivo by delaying the onset of symptoms, reducing the clinical score and decreasing T cell infiltration into the central nervous system (CNS) (Fig. 6A); however, it also influenced the survival of mice when injected at 2 mg/kg every alternate day (data not shown). A careful structural analysis revealed possible in vivo toxicity due to the trichloride (-Cl_3) motif present in compound 5D. Thus, various structural analogues of compound 5D lacking this motif were examined for blocking SOCE. This study identified compound 5J-4, which showed a strong block of SOCE in HeLa-O+S cells as well as endogenous SOCE in T_H17 cells, comparable to that observed with compound 5D (Fig. 6B and C). Moreover, in vivo injection of 2 mg/kg of compound 5J-4 every alternate day did not cause any lethality in mice (Suppl. Fig. 3A). Injection of compound 5J-4 into MOG_{35-55} peptide-immunized mice dramatically reduced the symptoms and delayed the onset of EAE demonstrating its protective effects on autoimmunity (Fig. 6D and Suppl. Fig. 3B). Consistent with the clinical score, infiltrated mononuclear cell numbers into the CNS was reduced and in particular, the infiltrated $CD4^+$ population was significantly decreased (Fig. 6E and Suppl. Fig. 3C). Next, we examined cytokine production by the mononuclear cells isolated from the draining lymph nodes and CNS of compound 5J-4 treated animals. In support of our in vitro and ex vivo data, we observed a predominant reduction in IL-$17A^+$ population, while that of IFN-γ^+ cells was not significantly reduced (Fig. 7A). While a majority of compound 5J-4-treated mice (~70%) exhibited this phenotype, there was a population of ~30% animals that showed a strong resistance to EAE and correspondingly reduction in both IFN-γ^+ and IL-$17A^+$ population of cells (data not shown). This phenotype could be due to variation in immunization efficacy or response of individual animals. To examine if reduced infiltration of T cells in the CNS was caused by a decrease in T cell differentiation, we analyzed the function of inflammatory T cells from the draining lymph nodes of control and 5J-4-injected mice. The mRNA levels of RORα and RORγt were dramatically reduced while those of T-bet and Foxp3 were not significantly affected (Suppl. Fig. 3D). These results suggest that, consistent with in vitro observations, injection of compound 5J-4 interfered with T cell differentiation after immunization that led to reduced numbers of inflammatory T cells into the CNS of EAE-induced mice. To examine whether CRAC channel function is important for sustained expression of IL-17A even in human $CD4^+$ T cells, we stimulated human peripheral blood mononuclear cells (PBMCs), and cultured them under T_H17-expanding conditions by inclusion of IL-1β, IL-23, and IL-2. In the control cells, we observed expression of both IFN-γ and IL-17A from $CD4^+$ T cells (Fig. 7B, left plot). Importantly, blocking of CRAC channels led to more than 50% reduction in IL-$17A^+$ population with little effect on IFN-γ^+ cells (Fig. 7B, graphs). These results demonstrate that CRAC channels have an important role in maintenance and expansion of human T_H17 population, similar to murine T_H17 cells.

NIH-PA Author Manuscript

NIH-PA Author Manuscript

NIH-PA Author Manuscript

Discussion

In this study, we identified a novel class of CRAC channel blockers using high throughput chemical library screen and asked how inhibition of Ca^{2+} signaling during TCR stimulation influenced differentiation and effector functions of T cells in vitro and in vivo. Using a combination of NFAT translocation as readout and a cell-line harboring amplified CRAC currents, we identified a novel class of immunomodulators, compound 5 and its analogues. A more potent analog of the lead compound, compound 5D, blocked CRAC currents generated by WT Orai1 and a constitutively active mutant of Orai1 without affecting Orai1 and STIM1 translocation, indicating that the blocking mechanism directly involves the pore-forming subunit, Orai1. Further studies of CRAC current inhibition showed block by extracellular, but not intracellular, application of compound 5D, suggesting that the binding site is accessible only from the extracellular face of Orai1. Comprehensive mutational analysis of all the residues with possible exposure to the extracellular milieu identified the putative channel gate V102 to be important for the blocking activity of compound 5D. Furthermore, compound 5D blocked SOCE mediated by all the Orai proteins, however, that by TrpC1 remained unaffected, indicating a specific block of CRAC channel activity (Fig. 1 and Suppl. Fig. 1).

After differentiation, effector T cells become activated by secondary engagement of TCR to produce cytokines in a Ca^{2+}-NFAT signaling-dependent manner. Thus, blocking CRAC channel activity was expected to reduce cytokine production upon secondary engagement of TCR in effector T cells (Fig. 2A, B, and C). Interestingly, blocking CRAC channels also had an inhibitory effect on naïve T cell differentiation upon first engagement of TCR, with preferential inhibition of T_H17 differentiation, and, to a lesser extent, T_H1 and T_H2 differentiation (Fig. 2D and E). Previously, we showed that Orai1-deficient T cells cultured under T_H1 and T_H2-polarizing conditions showed a pronounced reduction in expression of IFN-γ and IL-4, respectively (13). While reduction in IFN-γ levels is similar in both compound 5D-treated or Orai1-deficient T_H1 cells, that of IL-4 is less pronounced in compound 5D-treated T_H2 cells. This difference in T_H2 cells may be due to lack of Orai1 for the entire duration of differentiation as well as re-stimulation for cytokine production in Orai1-deficient T cells. Although it was previously shown that CNS-1 region in the Foxp3 promoter contains NFAT-binding element (50), inhibition of CRAC channel activity did not significantly influence development of inducible Tregs (Suppl. Fig. 2A). We do not know the exact reason for this discrepancy, but it is possible that the requirement for intracellular Ca^{2+} levels in Treg development is low and thus, the residual Ca^{2+} levels after blocker treatment may be sufficient for induction of Foxp3. This idea is further supported by the results from double knockout of STIM1 and STIM2 showing reduced levels of $Foxp3^+$ Tregs while individual knockouts did not affect Treg development (15).

T_H17 cells showed higher sensitivity to decreased levels of $[Ca^{2+}]_i$. At the current stage, the exact molecular mechanism behind this is not very clear. Previous studies have shown that upon antigen stimulation, T_H17 cells exhibit a distinct Ca^{2+} profile from T_H1 and T_H2 cells (36). T_H17 cells showed increased $[Ca^{2+}]_i$ with robust oscillations and correspondingly increased nuclear accumulation of NFAT for longer times than T_H2 cells (36). These data suggest that SOCE may play a more important role in differentiation of T_H17 cells than that of T_H1 and T_H2 cells. Specific usage of Ca^{2+} channels in different effector T cells was also observed in the studies of L-type voltage-gated Ca^{2+} (Ca_V1) channels. Administration of Ca_V1 blocker reduced T_H2 response but not T_H1 response in vitro and in vivo (51). Our data with CRAC channel blockers strongly support all these observations. Firstly, moderate concentration of compound 5D (1 μM) reduced SOCE by more than 85% in T_H17 cells, whereas the block was <50% in T_H1 cells (Fig. 2A). Since Orai proteins are known to heteromultimerize, the subunit stoichiometry and/or expression levels of Orai family

NIH-PA Author Manuscript

NIH-PA Author Manuscript

NIH-PA Author Manuscript

members may contribute to the higher reduction in SOCE in T_H17 cells. Secondly, it is possible that T_H17 differentiation may exhibit higher dependence on the Orai-NFAT pathway. Previous studies had predicted putative NFAT-binding elements on the RORγt promoter (45, 46) and an involvement of NFAT in IL-17, IL-21, and IL-22 production in T_H17 cells (48, 52). We also observed recruitment of NFAT onto the promoters and enhancers of RORα, RORγt, and IL-17A, which was reduced in compound 5D-treated or Orai1-deficient T cells (Figs. 4 and 5). Consistent with these studies, blocking NFAT translocation using cyclosporine A reduced expression of RORα and RORγt in T cells cultured under T_H17-polarizing conditions (Fig. 3C). Conversely, expression of CA-NFAT showed a strong rescue of the expression of RORα and RORγt in both, compound 5D-treated and Orai1-deficient T_H17 cells (Figs. 3 and 5). Another unexplored possibility is; in addition to regulating NFAT activity, Ca^{2+} signaling may play an important role in activating other signaling pathway(s) important for T_H17 differentiation. Signaling pathways at the early stage of T cell differentiation such as TCR stimulation in conjugation with T_H17-polarizing cytokines may be involved in pre-conditioning of epigenetic status of chromatin for further lineage-specific differentiation, and Ca^{2+} signaling triggered by TCR stimulation can be a part of these early TCR stimulation-triggered signaling pathways. Future experiments examining epigenetic modifications in wild-type and Orai1-deficient T_H17 cells can help in uncovering this hypothesis.

Notably, the blocking effect of compound 5D had selective inhibitory effects on the expression levels of RORα and RORγt, not on other transcription factors important for T_H17 differentiation (Fig. 2E and Suppl. Fig. 2C). Exogenous expression of RORα and RORγt could significantly reverse the inhibitory effect of compound 5D on IL-17A production (Fig. 3B). In addition, the inhibitory effect of CRAC channel blocker on IL-17 production did not show a strong correlation with the cell division rate (Fig. 3A). Therefore, contrary to the general concept that blocking Ca^{2+} signaling triggered by TCR stimulation leads to inhibition of T cell proliferation followed by suppression of T cell differentiation, inhibition of Orai1 activity suppresses selective signaling pathways important for T_H17 differentiation. Previous studies of transcriptional regulation of RORα and RORγt promoters have suggested an important role for STAT3 and c-Rel transcription factors. Durant et al used genome-wide ChIP and parallel sequencing (ChIP-seq) experiments from wild-type and STAT3-deficient T cells cultured under T_H17-polarizing condition and identified recruitment of STAT3 to both RORα and RORγt promoters (53). Consequently, expression levels of RORα and RORγt were significantly reduced in STAT3-deficient T cells. More recently, using ChIP and luciferase reporter assays, Ruan et al have shown a direct regulation of RORγt expression by c-Rel (46). Furthermore, the authors also observed reduced expression of RORα transcripts in c-Rel deficient T cells. Our studies now add another transcription factor, NFAT as a direct regulator of both RORα and RORγt expression. Contrary to T_H1 and T_H2 cells, T_H17 cells have intrinsic instability as demonstrated by extended in vitro culture or adoptive transfer (54). In addition to differentiation, maintenance of IL-17 production needs continued expression of RORγt controlled by IL-6, IL-21, and IL-23 (55, 56). Orai1-mediated Ca^{2+} signaling is not only required for differentiation but also important for maintenance and expansion of T_H17 cells. When compound 5D was included during the maintenance and expansion of pre-differentiated T_H17 cells ex vivo, a strong suppression of IL-17 production was observed (Fig. 2F). These results suggest that in addition to STAT3-inducing cytokines, high levels of Ca^{2+} signaling triggered by TCR stimulation is required for stable maintenance of T_H17 cells to reduce plasticity.

Consistent with the results from in vitro experiments, Orai1 blockers had a potent anti-inflammatory effect in vivo. Compound 5D or 5J-4 treatment blocked infiltration of T cells into the CNS and reduced IL-17-producing cells as well as expression of RORα and RORγt

NIH-PA Author Manuscript

NIH-PA Author Manuscript

NIH-PA Author Manuscript

(Figs. 6 and 7). The expression levels of Foxp3 was not dramatically changed in either in vitro or in vivo experimental settings (Suppl. Fig. 2A and 3D). These observations lead into an interesting hypothesis that highly inflammatory T cells such as T_H17 require high Ca^{2+} levels for their generation and maintenance while the Ca^{2+} requirement for other effector and regulatory T cells are moderate and low, respectively.

Recent screening studies have identified various small molecules that block the function of inflammatory T cells. Digoxin and its derivatives were identified from a small molecule library screen using transcriptional activity of RORγt as readout (57). In addition, a synthetic ligand, SR1001 was also identified as a blocker for the transcriptional activities of RORγt and RORα (58). Both these small molecule blockers showed protective effects on EAE. The molecular mechanism of the anti-inflammatory effect of another small molecule halofuginone was recently elucidated. Instead of acting on orphan receptors directly, halofuginone was shown to activate the amino acid starvation response (AAR) pathway (59). Halofuginone influenced the functions of T_H1, T_H2, and T_H17 cells at high concentrations; however, it selectively suppressed cytokine production by T_H17 cells at low concentrations and ameliorated the symptoms of EAE when administered in vivo. Although the outcomes of these small molecules are similar (e.g. anti-inflammatory effects), their working mechanisms are distinct from each other. CRAC channel blockers can be considered as general immunosuppressants taking into account their broad role in various immune cells. Earlier, a pyrazole derivative and RO2959 were identified as CRAC channel blockers and were shown to have high potency to suppress T cell function in vitro (60-62). However, our results suggest that compound 5D and its derivatives can have a stronger blocking effect on inflammatory T_H17 cells than other T cell subsets suggesting their potential usage in selective T cell subsets.

Human patients with non-functional CRAC channels suffer from fatal SCID, which can be rescued by bone marrow transplantation (63). These studies suggest a predominant role for CRAC channels in immune cells. Hence, blockers of CRAC channels are likely to have fewer side effects than widely used immunosuppressive drugs such as cyclosporin A and tacrolimus that block calcineurin activity. Our studies reveal that small molecule blockers of CRAC channels can provide a molecular probe to examine the role of Ca^{2+} signaling in the immune system, and potentially lead to novel and improved therapeutic approaches to suppress hypersensitive immune responses by blocking cytokine production in a short term and reducing differentiation and survival/expansion of inflammatory T cells in a long term.

Supplementary Material

Refer to Web version on PubMed Central for supplementary material.

Acknowledgments

We thank staff members of Molecular Screening Shared Resources and UCLA JCCC Flow Cytometry Core Facility for their technical help. We thank Drs. Ernest Wright and Kenneth Philipson for advice on the current project.

This work was supported by National Institute of Health grants AI-083432 and AI-101569, a grant from the Lupus Research Institute (Y.G.), and a scientist development grant from the American Heart Association, 12SDG12040188 (S.S.). Flow cytometry was performed in the UCLA JCCC Flow cytometry Core Facility supported by National Institute of Health grants CA-16042 and AI-28697.

References

1. Lewis RS. Store-operated calcium channels: new perspectives on mechanism and function. Cold Spring Harb Perspect Biol. 2011; 3:a003970. [PubMed: 21791698]

NIH-PA Author Manuscript

NIH-PA Author Manuscript

NIH-PA Author Manuscript

2. Srikanth S, Gwack Y. Orai1-NFAT signalling pathway triggered by T cell receptor stimulation. Mol Cells. 2013; 35:182–194. [PubMed: 23483280]
3. Zhang SL, Yeromin AV, Zhang XH, Yu Y, Safrina O, Penna A, Roos J, Stauderman KA, Cahalan MD. Genome-wide RNAi screen of Ca(2+) influx identifies genes that regulate Ca(2+) release-activated Ca(2+) channel activity. Proc Natl Acad Sci U S A. 2006; 103:9357–9362. [PubMed: 16751269]
4. Vig M, Peinelt C, Beck A, Koomoa DL, Rabah D, Koblan-Huberson M, Kraft S, Turner H, Fleig A, Penner R, Kinet JP. CRACM1 is a plasma membrane protein essential for store-operated Ca2+ entry. Science. 2006; 312:1220–1223. [PubMed: 16645049]
5. Feske S, Gwack Y, Prakriya M, Srikanth S, Puppel SH, Tanasa B, Hogan PG, Lewis RS, Daly M, Rao A. A mutation in Orai1 causes immune deficiency by abrogating CRAC channel function. Nature. 2006; 441:179–185. [PubMed: 16582901]
6. Gwack Y, Srikanth S, Feske S, Cruz-Guilloty F, Oh-hora M, Neems DS, Hogan PG, Rao A. Biochemical and functional characterization of Orai proteins. J Biol Chem. 2007; 282:16232–16243. [PubMed: 17293345]
7. Liou J, Kim ML, Heo WD, Jones JT, Myers JW, Ferrell JE Jr. Meyer T. STIM is a Ca2+ sensor essential for Ca2+-store-depletion-triggered Ca2+ influx. Curr Biol. 2005; 15:1235–1241. [PubMed: 16005298]
8. Roos J, DiGregorio PJ, Yeromin AV, Ohlsen K, Lioudyno M, Zhang S, Safrina O, Kozak JA, Wagner SL, Cahalan MD, Velicelebi G, Stauderman KA. STIM1, an essential and conserved component of store-operated Ca2+ channel function. J Cell Biol. 2005; 169:435–445. [PubMed: 15866891]
9. Zhang SL, Yu Y, Roos J, Kozak JA, Deerinck TJ, Ellisman MH, Stauderman KA, Cahalan MD. STIM1 is a Ca2+ sensor that activates CRAC channels and migrates from the Ca2+ store to the plasma membrane. Nature. 2005; 437:902–905. [PubMed: 16208375]
10. Liou J, Fivaz M, Inoue T, Meyer T. Live-cell imaging reveals sequential oligomerization and local plasma membrane targeting of stromal interaction molecule 1 after Ca2+ store depletion. Proc Natl Acad Sci U S A. 2007; 104:9301–9306. [PubMed: 17517596]
11. Putney JW Jr. A model for receptor-regulated calcium entry. Cell Calcium. 1986; 7:1–12. [PubMed: 2420465]
12. Picard C, McCarl CA, Papolos A, Khalil S, Luthy K, Hivroz C, LeDeist F, Rieux-Laucat F, Rechavi G, Rao A, Fischer A, Feske S. STIM1 mutation associated with a syndrome of immunodeficiency and autoimmunity. N Engl J Med. 2009; 360:1971–1980. [PubMed: 19420366]
13. Gwack Y, Srikanth S, Oh-Hora M, Hogan PG, Lamperti ED, Yamashita M, Gelinas C, Neems DS, Sasaki Y, Feske S, Prakriya M, Rajewsky K, Rao A. Hair loss and defective T- and B-cell function in mice lacking ORAI1. Mol Cell Biol. 2008; 28:5209–5222. [PubMed: 18591248]
14. Matsumoto M, Fujii Y, Baba A, Hikida M, Kurosaki T, Baba Y. The calcium sensors STIM1 and STIM2 control B cell regulatory function through interleukin-10 production. Immunity. 2011; 34:703–714. [PubMed: 21530328]
15. Oh-Hora M, Yamashita M, Hogan PG, Sharma S, Lamperti E, Chung W, Prakriya M, Feske S, Rao A. Dual functions for the endoplasmic reticulum calcium sensors STIM1 and STIM2 in T cell activation and tolerance. Nat Immunol. 2008; 9:432–443. [PubMed: 18327260]
16. Schuhmann MK, Stegner D, Berna-Erro A, Bittner S, Braun A, Kleinschnitz C, Stoll G, Wiendl H, Meuth SG, Nieswandt B. Stromal interaction molecules 1 and 2 are key regulators of autoreactive T cell activation in murine autoimmune central nervous system inflammation. J Immunol. 2010; 184:1536–1542. [PubMed: 20028655]
17. Vig M, DeHaven WI, Bird GS, Billingsley JM, Wang H, Rao PE, Hutchings AB, Jouvin MH, Putney JW, Kinet JP. Defective mast cell effector functions in mice lacking the CRACM1 pore subunit of store-operated calcium release-activated calcium channels. Nat Immunol. 2008; 9:89–96. [PubMed: 18059270]
18. Bettelli E, Carrier Y, Gao W, Korn T, Strom TB, Oukka M, Weiner HL, Kuchroo VK. Reciprocal developmental pathways for the generation of pathogenic effector TH17 and regulatory T cells. Nature. 2006; 441:235–238. [PubMed: 16648838]

NIH-PA Author Manuscript

NIH-PA Author Manuscript

NIH-PA Author Manuscript

19. Veldhoen M, Hocking RJ, Atkins CJ, Locksley RM, Stockinger B. TGFbeta in the context of an inflammatory cytokine milieu supports de novo differentiation of IL-17-producing T cells. Immunity. 2006; 24:179–189. [PubMed: 16473830]
20. Korn T, Bettelli E, Oukka M, Kuchroo VK. IL-17 and Th17 Cells. Annu Rev Immunol. 2009; 27:485–517. [PubMed: 19132915]
21. Zhou L, Littman DR. Transcriptional regulatory networks in Th17 cell differentiation. Curr Opin Immunol. 2009; 21:146–152. [PubMed: 19328669]
22. O'Shea JJ, Lahesmaa R, Vahedi G, Laurence A, Kanno Y. Genomic views of STAT function in CD4+ T helper cell differentiation. Nat Rev Immunol. 2011; 11:239–250. [PubMed: 21436836]
23. Dong C. TH17 cells in development: an updated view of their molecular identity and genetic programming. Nat Rev Immunol. 2008; 8:337–348. [PubMed: 18408735]
24. Yang XO, Pappu BP, Nurieva R, Akimzhanov A, Kang HS, Chung Y, Ma L, Shah B, Panopoulos AD, Schluns KS, Watowich SS, Tian Q, Jetten AM, Dong C. T helper 17 lineage differentiation is programmed by orphan nuclear receptors ROR alpha and ROR gamma. Immunity. 2008; 28:29–39. [PubMed: 18164222]
25. Constant SL, Bottomly K. Induction of Th1 and Th2 CD4+ T cell responses: the alternative approaches. Annu Rev Immunol. 1997; 15:297–322. [PubMed: 9143690]
26. Gwack Y, Sharma S, Nardone J, Tanasa B, Iuga A, Srikanth S, Okamura H, Bolton D, Feske S, Hogan PG, Rao A. A genome-wide Drosophila RNAi screen identifies DYRK-family kinases as regulators of NFAT. Nature. 2006; 441:646–650. [PubMed: 16511445]
27. Srikanth S, Jung HJ, Kim KD, Souda P, Whitelegge J, Gwack Y. A novel EF-hand protein, CRACR2A, is a cytosolic Ca2+ sensor that stabilizes CRAC channels in T cells. Nat Cell Biol. 2010; 12:436–446. [PubMed: 20418871]
28. Srikanth S, Jew M, Kim KD, Yee MK, Abramson J, Gwack Y. Junctate is a Ca2+-sensing structural component of Orai1 and stromal interaction molecule 1 (STIM1). Proc Natl Acad Sci U S A. 2012; 109:8682–8687. [PubMed: 22586105]
29. Srikanth S, Yee MK, Gwack Y, Ribalet B. The third transmembrane segment of orai1 protein modulates Ca2+ release-activated Ca2+ (CRAC) channel gating and permeation properties. J Biol Chem. 2011; 286:35318–35328. [PubMed: 21865174]
30. McNally BA, Yamashita M, Engh A, Prakriya M. Structural determinants of ion permeation in CRAC channels. Proc Natl Acad Sci U S A. 2009; 106:22516–22521. [PubMed: 20018736]
31. Zhou Y, Ramachandran S, Oh-Hora M, Rao A, Hogan PG. Pore architecture of the ORAI1 store-operated calcium channel. Proc Natl Acad Sci U S A. 2010; 107:4896–4901. [PubMed: 20194792]
32. McNally BA, Somasundaram A, Yamashita M, Prakriya M. Gated regulation of CRAC channel ion selectivity by STIM1. Nature. 2012; 482:241–245. [PubMed: 22278058]
33. Kim KD, Srikanth S, Yee MK, Mock DC, Lawson GW, Gwack Y. ORAI1 deficiency impairs activated T cell death and enhances T cell survival. J Immunol. 2011; 187:3620–3630. [PubMed: 21873530]
34. DeHaven WI, Smyth JT, Boyles RR, Putney JW Jr. Calcium inhibition and calcium potentiation of Orai1, Orai2, and Orai3 calcium release-activated calcium channels. J Biol Chem. 2007; 282:17548–17556. [PubMed: 17452328]
35. Lis A, Peinelt C, Beck A, Parvez S, Monteilh-Zoller M, Fleig A, Penner R. CRACM1, CRACM2, and CRACM3 are store-operated Ca2+ channels with distinct functional properties. Curr Biol. 2007; 17:794–800. [PubMed: 17442569]
36. Weber KS, Miller MJ, Allen PM. Th17 cells exhibit a distinct calcium profile from Th1 and Th2 cells and have Th1-like motility and NF-AT nuclear localization. J Immunol. 2008; 180:1442–1450. [PubMed: 18209039]
37. Serfling E, Avots A, Klein-Hessling S, Rudolf R, Vaeth M, Berberich-Siebelt F. NFATc1/alphaA: The other Face of NFAT Factors in Lymphocytes. Cell Commun Signal. 2012; 10:16. [PubMed: 22764736]
38. Bauquet AT, Jin H, Paterson AM, Mitsdoerffer M, Ho IC, Sharpe AH, Kuchroo VK. The costimulatory molecule ICOS regulates the expression of c-Maf and IL-21 in the development of follicular T helper cells and TH-17 cells. Nat Immunol. 2009; 10:167–175. [PubMed: 19098919]

NIH-PA Author Manuscript NIH-PA Author Manuscript NIH-PA Author Manuscript

39. Brustle A, Heink S, Huber M, Rosenplanter C, Stadelmann C, Yu P, Arpaia E, Mak TW, Kamradt T, Lohoff M. The development of inflammatory T(H)-17 cells requires interferon-regulatory factor 4. Nat Immunol. 2007; 8:958–966. [PubMed: 17676043]
40. Chen Z, Laurence A, Kanno Y, Pacher-Zavisin M, Zhu BM, Tato C, Yoshimura A, Hennighausen L, O'Shea JJ. Selective regulatory function of Socs3 in the formation of IL-17-secreting T cells. Proc Natl Acad Sci U S A. 2006; 103:8137–8142. [PubMed: 16698929]
41. Dang EV, Barbi J, Yang HY, Jinasena D, Yu H, Zheng Y, Bordman Z, Fu J, Kim Y, Yen HR, Luo W, Zeller K, Shimoda L, Topalian SL, Semenza GL, Dang CV, Pardoll DM, Pan F. Control of T(H)17/T(reg) balance by hypoxia-inducible factor 1. Cell. 2011; 146:772–784. [PubMed: 21871655]
42. Schraml BU, Hildner K, Ise W, Lee WL, Smith WA, Solomon B, Sahota G, Sim J, Mukasa R, Cemerski S, Hatton RD, Stormo GD, Weaver CT, Russell JH, Murphy TL, Murphy KM. The AP-1 transcription factor Batf controls T(H)17 differentiation. Nature. 2009; 460:405–409. [PubMed: 19578362]
43. Veldhoen M, Hirota K, Westendorf AM, Buer J, Dumoutier L, Renauld JC, Stockinger B. The aryl hydrocarbon receptor links TH17-cell-mediated autoimmunity to environmental toxins. Nature. 2008; 453:106–109. [PubMed: 18362914]
44. Zhang F, Meng G, Strober W. Interactions among the transcription factors Runx1, RORgammat and Foxp3 regulate the differentiation of interleukin 17-producing T cells. Nat Immunol. 2008; 9:1297–1306. [PubMed: 18849990]
45. Xi H, Schwartz R, Engel I, Murre C, Kersh GJ. Interplay between RORgammat, Egr3, and E proteins controls proliferation in response to pre-TCR signals. Immunity. 2006; 24:813–826. [PubMed: 16782036]
46. Ruan Q, Kameswaran V, Zhang Y, Zheng S, Sun J, Wang J, Devirgiliis J, Liou HC, Beg AA, Chen YH. The Th17 immune response is controlled by the Rel-ROR{gamma}-ROR{gamma}T transcriptional axis. J Exp Med. 2011; 208:2321–2333. [PubMed: 22006976]
47. Ghosh S, Koralov SB, Stevanovic I, Sundrud MS, Sasaki Y, Rajewsky K, Rao A, Muller MR. Hyperactivation of nuclear factor of activated T cells 1 (NFAT1) in T cells attenuates severity of murine autoimmune encephalomyelitis. Proc Natl Acad Sci U S A. 2010; 107:15169–15174. [PubMed: 20696888]
48. Gomez-Rodriguez J, Sahu N, Handon R, Davidson TS, Anderson SM, Kirby MR, August A, Schwartzberg PL. Differential expression of interleukin-17A and -17F is coupled to T cell receptor signaling via inducible T cell kinase. Immunity. 2009; 31:587–597. [PubMed: 19818650]
49. Macian F, Garcia-Cozar F, Im SH, Horton HF, Byrne MC, Rao A. Transcriptional mechanisms underlying lymphocyte tolerance. Cell. 2002; 109:719–731. [PubMed: 12086671]
50. Tone Y, Furuuchi K, Kojima Y, Tykocinski ML, Greene MI, Tone M. Smad3 and NFAT cooperate to induce Foxp3 expression through its enhancer. Nat Immunol. 2008; 9:194–202. [PubMed: 18157133]
51. Badou A, Jha MK, Matza D, Flavell RA. Emerging Roles of L-Type Voltage-Gated and Other Calcium Channels in T Lymphocytes. Front Immunol. 2013; 4:243. [PubMed: 24009608]
52. Spolski R, Leonard WJ. Interleukin-21: basic biology and implications for cancer and autoimmunity. Annu Rev Immunol. 2008; 26:57–79. [PubMed: 17953510]
53. Durant L, Watford WT, Ramos HL, Laurence A, Vahedi G, Wei L, Takahashi H, Sun HW, Kanno Y, Powrie F, O'Shea JJ. Diverse targets of the transcription factor STAT3 contribute to T cell pathogenicity and homeostasis. Immunity. 2010; 32:605–615. [PubMed: 20493732]
54. Mukasa R, Balasubramani A, Lee YK, Whitley SK, Weaver BT, Shibata Y, Crawford GE, Hatton RD, Weaver CT. Epigenetic instability of cytokine and transcription factor gene loci underlies plasticity of the T helper 17 cell lineage. Immunity. 2010; 32:616–627. [PubMed: 20471290]
55. Kanno Y, Vahedi G, Hirahara K, Singleton K, O'Shea JJ. Transcriptional and epigenetic control of T helper cell specification: molecular mechanisms underlying commitment and plasticity. Annu Rev Immunol. 2012; 30:707–731. [PubMed: 22224760]
56. Wilson CB, Rowell E, Sekimata M. Epigenetic control of T-helper-cell differentiation. Nat Rev Immunol. 2009; 9:91–105. [PubMed: 19151746]

NIH-PA Author Manuscript

NIH-PA Author Manuscript

NIH-PA Author Manuscript

57. Huh JR, Leung MW, Huang P, Ryan DA, Krout MR, Malapaka RR, Chow J, Manel N, Ciofani M, Kim SV, Cuesta A, Santori FR, Lafaille JJ, Xu HE, Gin DY, Rastinejad F, Littman DR. Digoxin and its derivatives suppress TH17 cell differentiation by antagonizing RORgammat activity. Nature. 2011; 472:486–490. [PubMed: 21441909]

58. Solt LA, Kumar N, Nuhant P, Wang Y, Lauer JL, Liu J, Istrate MA, Kamenecka TM, Roush WR, Vidovic D, Schurer SC, Xu J, Wagoner G, Drew PD, Griffin PR, Burris TP. Suppression of TH17 differentiation and autoimmunity by a synthetic ROR ligand. Nature. 2011; 472:491–494. [PubMed: 21499262]

59. Sundrud MS, Koralov SB, Feuerer M, Calado DP, Kozhaya AE, Rhule-Smith A, Lefebvre RE, Unutmaz D, Mazitschek R, Waldner H, Whitman M, Keller T, Rao A. Halofuginone inhibits TH17 cell differentiation by activating the amino acid starvation response. Science. 2009; 324:1334–1338. [PubMed: 19498172]

60. Ishikawa J, Ohga K, Yoshino T, Takezawa R, Ichikawa A, Kubota H, Yamada T. A pyrazole derivative, YM-58483, potently inhibits store-operated sustained Ca2+ influx and IL-2 production in T lymphocytes. J Immunol. 2003; 170:4441–4449. [PubMed: 12707319]

61. Zitt C, Strauss B, Schwarz EC, Spaeth N, Rast G, Hatzelmann A, Hoth M. Potent inhibition of Ca2+ release-activated Ca2+ channels and T-lymphocyte activation by the pyrazole derivative BTP2. J Biol Chem. 2004; 279:12427–12437. [PubMed: 14718545]

62. Chen G, Panicker S, Lau KY, Apparsundaram S, Patel VA, Chen SL, Soto R, Jung JK, Ravindran P, Okuhara D, Bohnert G, Che Q, Rao PE, Allard JD, Badi L, Bitter HM, Nunn PA, Narula SK, DeMartino JA. Characterization of a novel CRAC inhibitor that potently blocks human T cell activation and effector functions. Mol Immunol. 2013; 54:355–367. [PubMed: 23357789]

63. Feske S. ORAI1 and STIM1 deficiency in human and mice: roles of store-operated Ca2+ entry in the immune system and beyond. Immunol Rev. 2009; 231:189–209. [PubMed: 19754898]

NIH-PA Author Manuscript
NIH-PA Author Manuscript
NIH-PA Author Manuscript

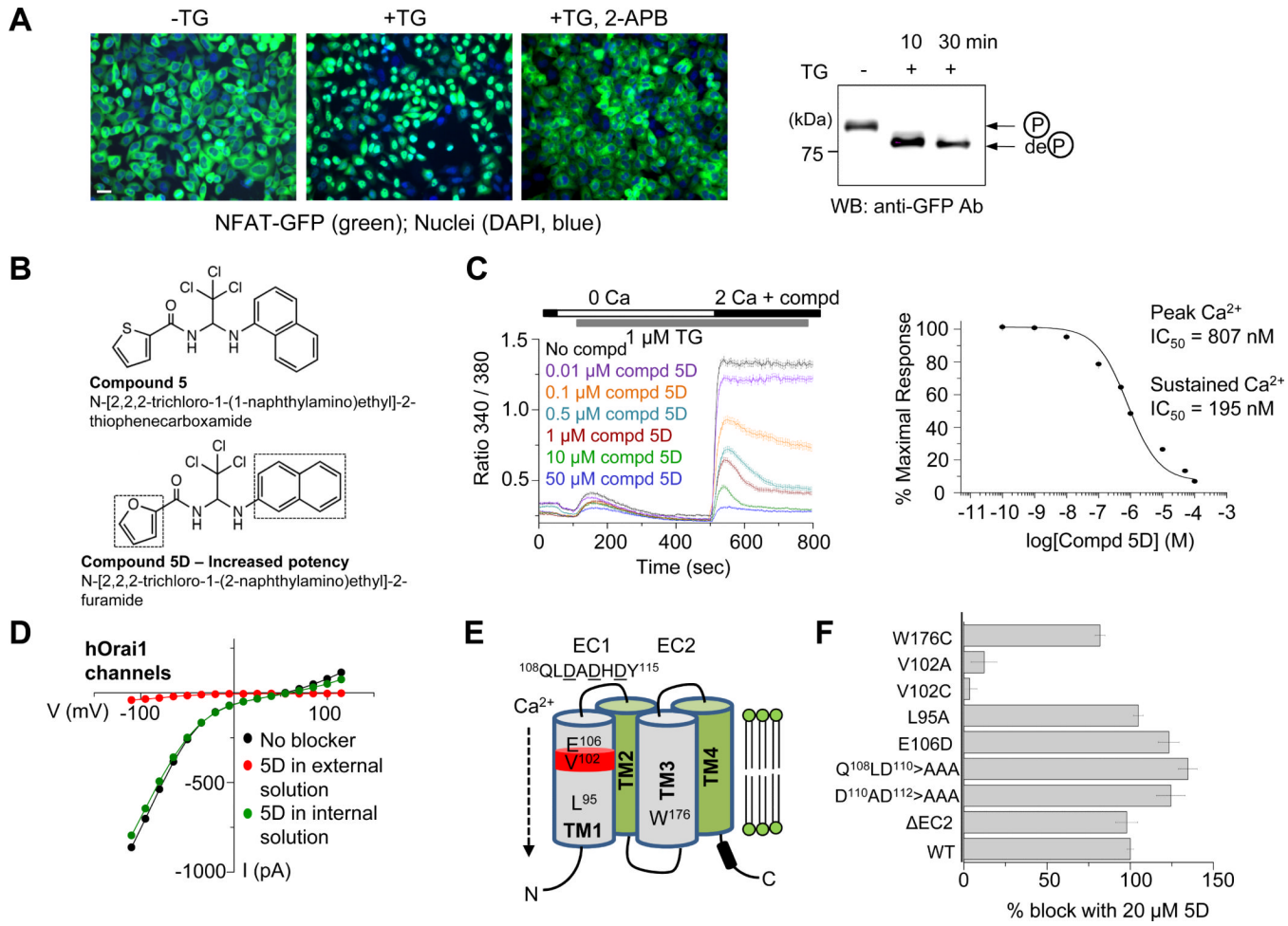

Figure 1. Identification of compound 5D as a small molecule blocker of CRAC channels

(**A**) Development of NFAT translocation as readout for high throughput screen. HeLa cells stably expressing Orai1, STIM1, and NFATc2 (1-460)-GFP, were left untreated (-TG) or treated with thapsigargin (+TG, 1 μM, 30 min) with and without 2-APB. The cells were examined by microscopy for nuclear accumulation of NFAT-GFP (left) or immunoblotting for dephosphorylation of NFAT with anti-GFP antibody (right). P, phosphorylated; deP, dephosphorylated; WB, western blotting. Scale bar – 10 μm.

(**B**) Chemical structures of compound 5 and its structural analogue compound 5D.

(**C**) Dose-dependent block of endogenous SOCE in primary murine effector T cells cultured under non-skewing conditions after exposure to compound 5D. Each trace represents average ± s.e.m from 50-60 primary T cells. The graph on the right shows dose-dependent block of sustained $[Ca^{2+}]_i$ by compound 5D with the indicated half-maximum inhibitory concentration (IC_{50}).

(**D**) Inhibition of CRAC currents by compound 5D. Measurement of CRAC currents from HEK293 cells co-expressing Orai1 and STIM1 (black trace). Cells were exposed to compound 5D (10 μM) by either intracellular (green trace) or extracellular (red trace) application. Representative I-V from at least four different cells in each condition is depicted.

(**E**) Schematic of Orai1. Orai1 contains four transmembrane segments (TM1-TM4) with its N and C terminus facing the cytoplasm, and two extracellular loops (EC1 and EC2). Residues L95, V102 and E106 in TM1 directly line the ion permeation pathway and V102

NIH-PA Author Manuscript

NIH-PA Author Manuscript

NIH-PA Author Manuscript

has been proposed to form the gate of the CRAC channel (marked in red). The D^{110}×D^{112}×D^{114} motif in the EC1 is important for ion selectivity of the channel and mutation of W176 in TM3 makes the channel constitutively open.
(**F**) Compound 5D-mediated block of SOCE induced by various mutants of Orai1. SOCE measurements and its block by compound 5D from Orai1$^{-/-}$ murine embryonic fibroblasts (MEFs) transduced with retroviruses encoding either wild-type (WT) or indicated mutants of Orai1. Residues deleted in the second extracellular loop (ΔEC) are described in Materials and Methods. Data represent average ± s.e.m from 25-35 fibroblasts and are normalized to the block of wild-type Orai1. The blocking effect of compound 5D on constitutively active channels such as W176C, V102A, and V102C was measured without store depletion.

NIH-PA Author Manuscript
NIH-PA Author Manuscript
NIH-PA Author Manuscript

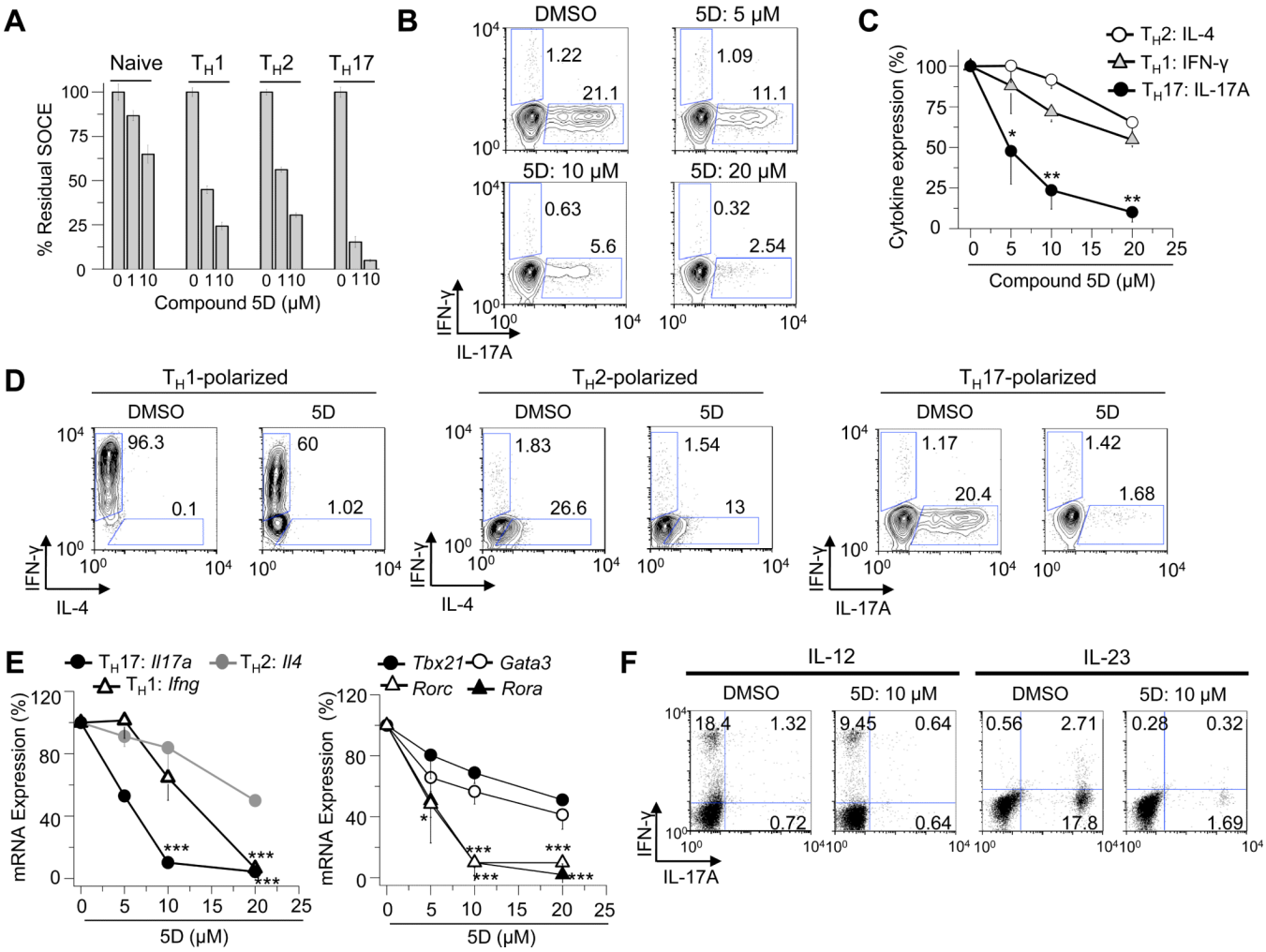

Figure 2. Inhibition of CRAC channels reduces differentiation of effector T cells

(**A**) Measurement of SOCE in naïve and indicated effector T cells in the absence and presence of 1 or 10 μM of compound 5D. Data represent average ± s.e.m of peak SOCE from 40-60 cells and are normalized to SOCE in the absence of compound 5D.

(**B**) Compound 5D-mediated inhibition of IL-17A production. Naïve T cells differentiated under T_H17-polarizing conditions and re-stimulated with PMA and ionomycin with different concentrations of compound 5D or DMSO (vehicle) were examined for IL-17A and IFN-γ production.

(**C**) Compound 5D-mediated inhibition of cytokine production by T_H1, T_H2, and T_H17 cells. Naïve T cells differentiated under T_H1-, T_H2-, or T_H17-polarizing conditions were stimulated with PMA and ionomycin after 4 days in the presence of different concentrations of compound 5D and examined for cytokine expression using intracellular staining. Data were normalized to cytokine levels of cells treated with DMSO.

(**D**) Compound 5D affects T cell differentiation. Naïve T cells differentiated under T_H1, T_H2, and T_H17-polarizing conditions in the absence or presence of compound 5D (15 μM) for four days were re-stimulated with PMA and ionomycin for 6 hrs in the absence of compound 5D and stained for IFN-γ, IL-4, and IL-17A, respectively.

(**E**) Compound 5D-mediated reduction in the expression of cytokines and transcription factors in T cells. Naïve T cells differentiated under T_H1, T_H2, and T_H17-polarizing conditions with compound 5D were washed, restimulated with PMA plus ionomycin, and

NIH-PA Author Manuscript

NIH-PA Author Manuscript

NIH-PA Author Manuscript

harvested for mRNA expression analyses of IFN-γ (T_H1 cells), IL-4 (T_H2 cells), and IL-17A (T_H17 cells) (left panel). In addition, the mRNA levels of T-bet, GATA-3, RORγt, and RORα were also measured under T_H1, T_H2, and T_H17-polarizing conditions, respectively (right panel). *P<0.05, ***P<0.0005.

(**F**) Compound 5D-mediated block of expansion and maintenance of pre-differentiated T_H17 cells. Cells were collected from draining lymph nodes of mice 7 days after immunization with MOG_{35-55}/CFA and cultured for four days with MOG_{35-55} peptide together with IL-12 or IL-23 in the presence of DMSO or 10 μM of compound 5D. $CD4^+$ T cells were examined for IL-17A and IFN-γ production after stimulation with PMA and ionomycin.

NIH-PA Author Manuscript

NIH-PA Author Manuscript

NIH-PA Author Manuscript

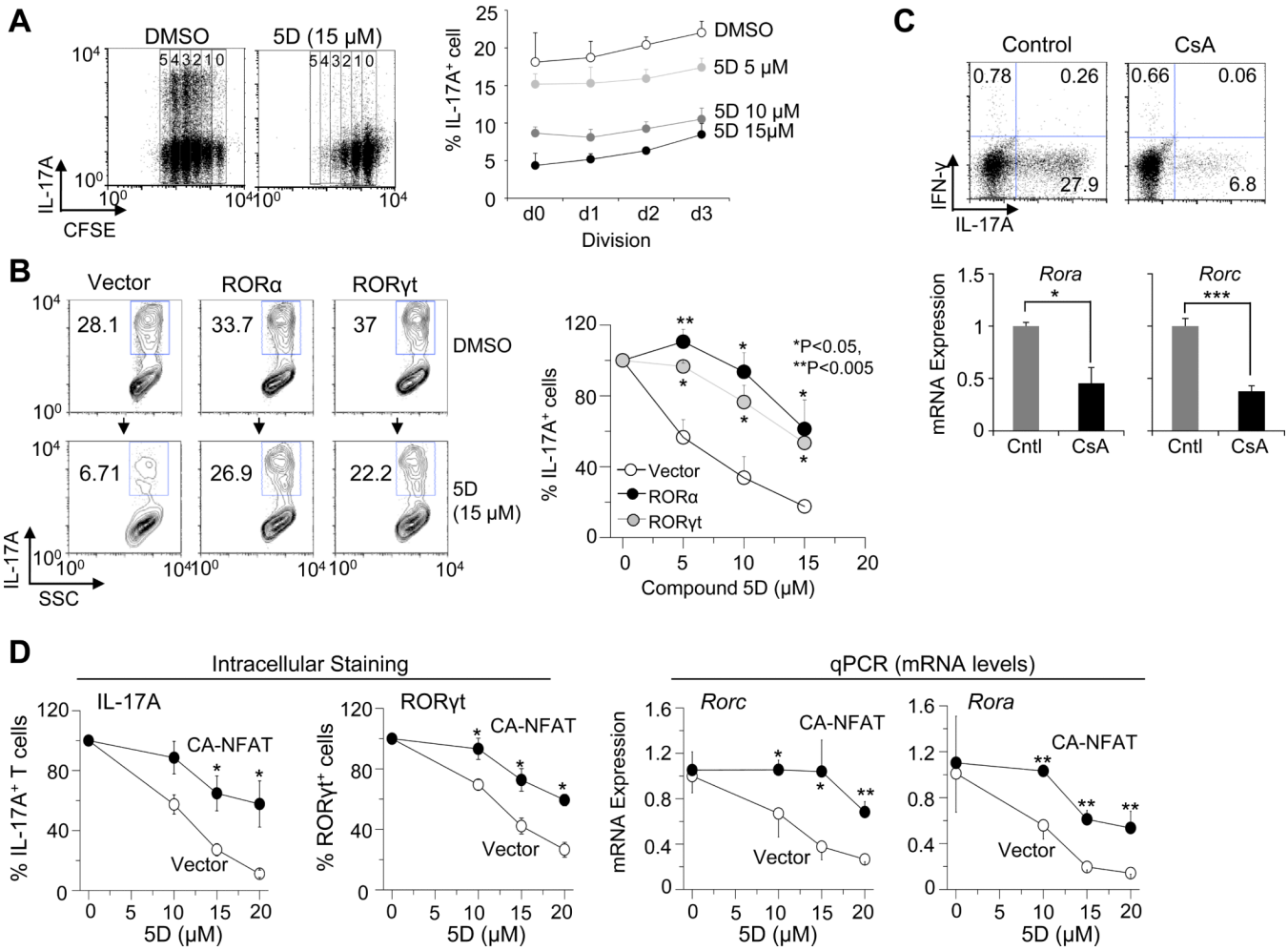

Figure 3. Ca^{2+} signaling mediated by Orai1 is important for NFAT-mediated expression of RORα and RORγt in T_H17 cells

(**A**) Compound 5D treatment reduces IL-17A production irrespective of blocking proliferation. CFSE-labeled naïve cells differentiated under T_H17-polarizing conditions with compound 5D were examined for IL-17A production in each division after 3 days of stimulation. Line graph shows average ± standard deviation from 3 independent experiments.

(**B**) Recovery of IL-17A$^+$ population by expression of RORα and RORγt in compound 5D-treated cells. Naïve T cells cultured under T_H17-polarizing conditions with compound 5D were transduced with retroviruses encoding RORα or RORγt, and examined for IL-17A production on day 4. Line graph on the right shows average ± s.e.m of IL-17A$^+$ population from four independent experiments.

(**C**) Cyclosporin A (CsA) treatment suppresses expression of IL-17A, RORα, and RORγt. Naïve T cells were cultured under T_H17-polarizing conditions with 5 nM cyclosporine A (CsA) for four days, washed, restimulated with PMA and ionomycin, and examined for production of IL-17A (top) and mRNA levels of RORα or RORγt (bottom). Intracellular staining data are representative of three independent experiments. Transcript analysis shows average ± standard deviation. Cntl – control.

(**D**) Expression of constitutively active NFAT rescues compound 5D-mediated inhibition of T_H17 differentiation. Naïve T cells cultured under T_H17-polarizing conditions with different concentrations of compound 5D were transduced with retroviruses encoding constitutively

active NFATc2 (CA-NFAT), and examined for IL-17A production and RORγt expression on day 4 using intracellular staining (left two panels). The same cells were also used for mRNA expression analysis of RORα or RORγt (right two panels). *P<0.05, **P<0.005.

NIH-PA Author Manuscript
NIH-PA Author Manuscript
NIH-PA Author Manuscript

NIH-PA Author Manuscript
NIH-PA Author Manuscript
NIH-PA Author Manuscript

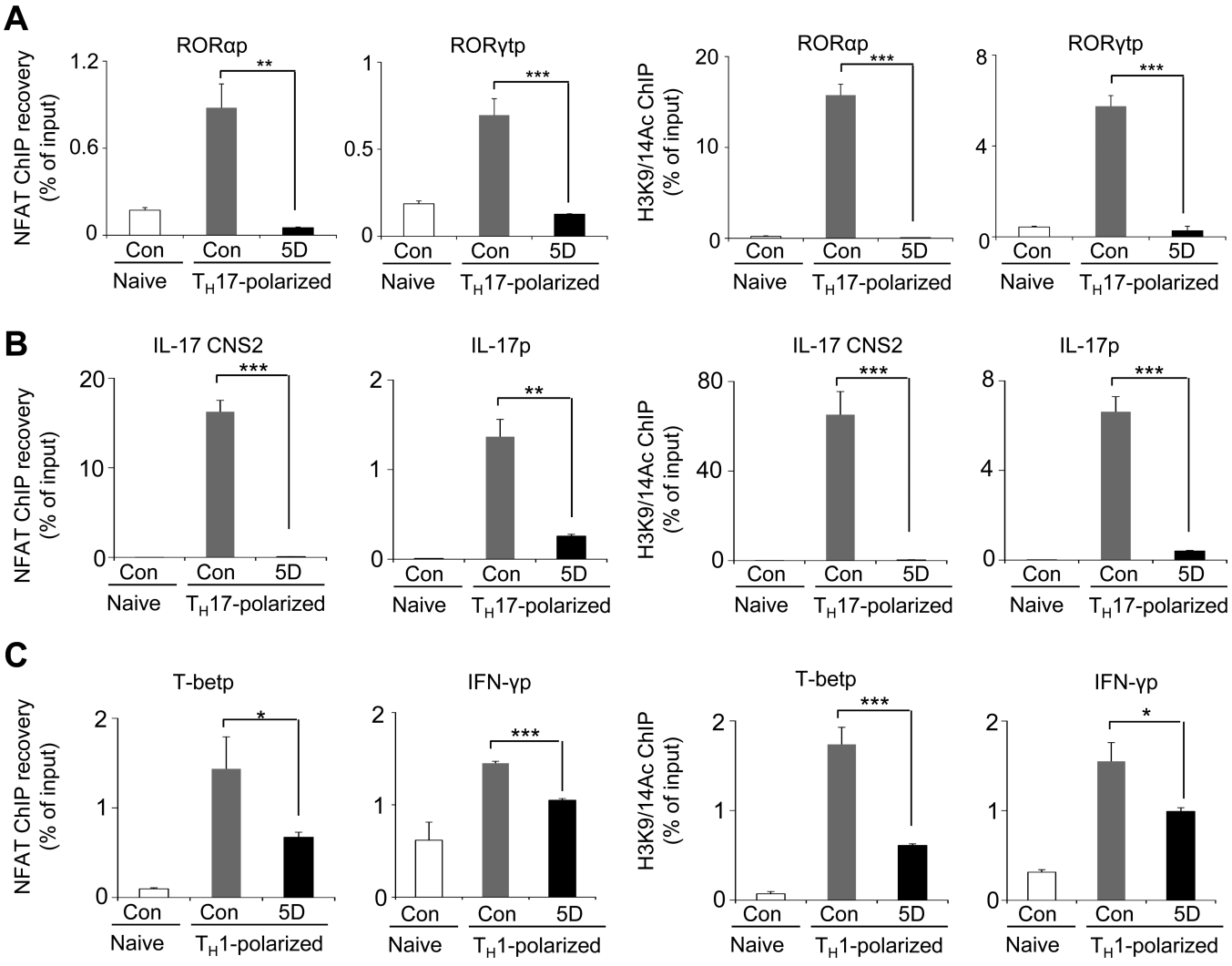

Figure 4. Ca^{2+} signaling mediated by Orai1 is important for NFAT-mediated expression of RORα and RORγt in T_H17 cells

(**A**) ChIP-PCR analysis of NFAT recruitment and acetylation of histone H3K9/14 at the promoters of RORα or RORγt. Real-time PCR quantification of RORα and RORγt promoter (RORαp and RORγtp) sequences after ChIP with antibody to NFATc2 (left two panels), and acetylated H3K9 and H3K14 (H3K9/14Ac, right two panels) in DMSO and compound 5D-treated cells after stimulation with anti-CD3 and anti-CD28 antibodies for 16 hours under T_H17-polarizing conditions. Data were normalized to the mean ChIP recovery of all experiments. *P<0.05, **P<0.005, ***P<0.0005.

(**B**) ChIP-PCR analysis of NFAT recruitment and acetylation of histone H3K9/14 at the promoter (IL-17p) and enhancer (CNS2) of IL-17A in the presence and absence of compound 5D. Naïve T cells were stimulated with anti-CD3 and anti-CD28 antibodies for 16 hours under T_H17-polarizing conditions.

(**C**) ChIP-PCR analysis of NFAT recruitment and acetylation of histone H3K9/14 at the promoters of T-bet and INF-γ. Quantitative RT-PCR analyses after ChIP with antibody to NFATc2 (left two panels) and acetylated H3K9 and H3K14 (H3K9/14Ac, right two panels) in DMSO and compound 5D-treated cells after stimulation with anti-CD3 and anti-CD28 antibodies for 16 hours under T_H1-polarizing conditions.

NIH-PA Author Manuscript
NIH-PA Author Manuscript
NIH-PA Author Manuscript

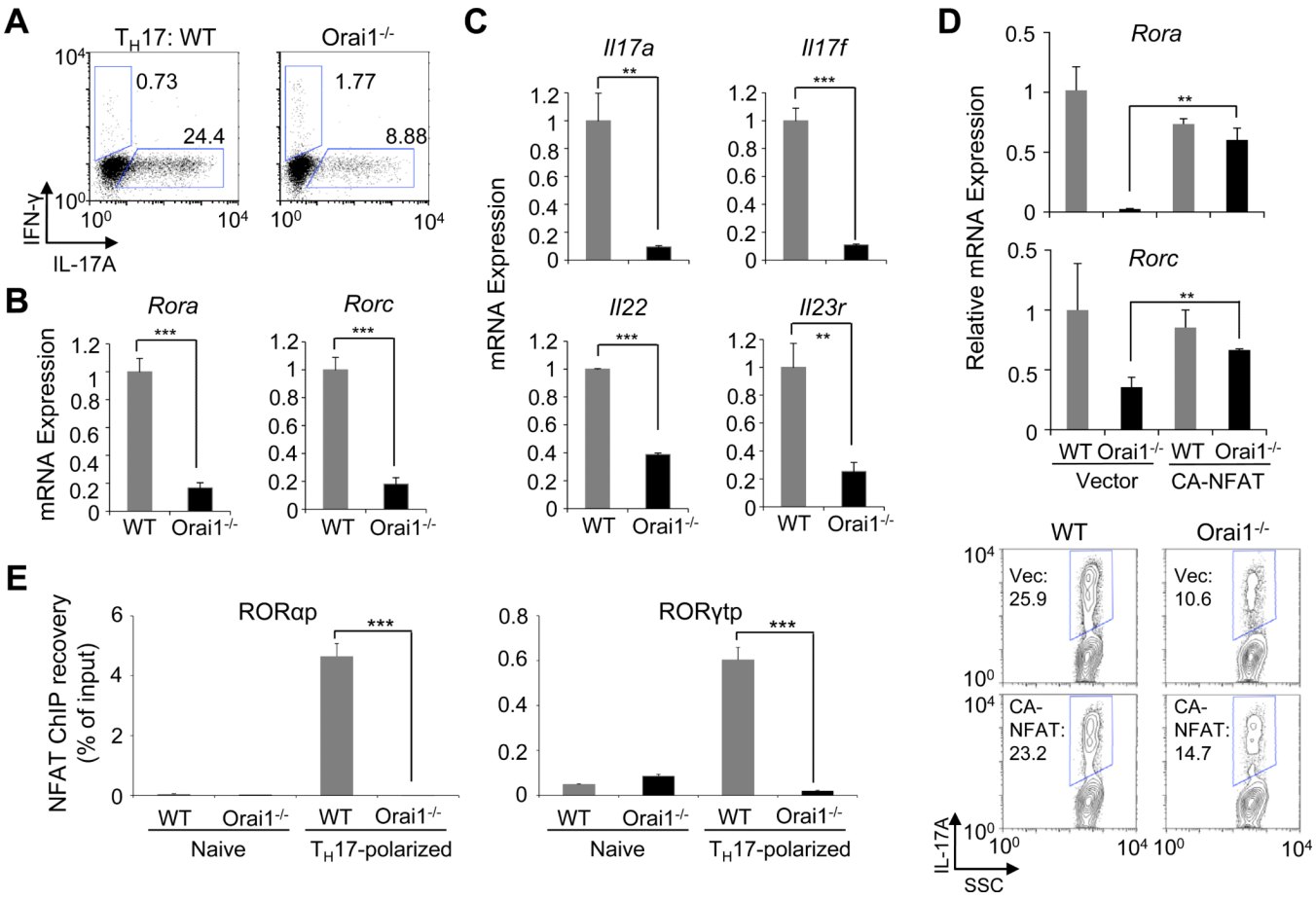

Figure 5. Orai1$^{-/-}$ T cells show a defect in T_H17 differentiation similar to that observed in compound 5D-treated cells

(**A**) Orai1$^{-/-}$ T cells show a defect in IL-17 production. Naïve CD4^{+} T Cells were stimulated and cultured under T_H17-polarizing conditions, restimulated with PMA and ionomycin after four days, and examined for IL-17A expression.

(**B**) mRNA expression analyses of RORα and RORγt in control and Orai1$^{-/-}$ T cells after stimulation with anti-CD3 and anti-CD28 antibodies under T_H17-polarizing conditions for four days.

(**C**) mRNA expression analyses in Orai1$^{-/-}$ T cells cultured under T_H17-polarizing conditions. WT and Orai1$^{-/-}$ naïve T cells cultured under T_H17-polarizing conditions for four days were stimulated with PMA and ionomycin, and analyzed for expression of indicated genes.

(**D**) Expression of CA-NFAT partially rescues T_H17 differentiation defect in Orai1$^{-/-}$ T cells. WT and Orai1$^{-/-}$ naïve T cells differentiated under T_H17-polarizing conditions were transduced with retroviruses encoding CA-NFAT, and examined for mRNA expression of RORα or RORγt (top panels) and IL-17A production (lower panels).

(**E**) ChIP-PCR analysis of NFAT recruitment onto the promoters of RORα or RORγt. Quantative RTPCR analysis of RORα and RORγt promoter (RORαp and RORγtp) sequences after ChIP recovery with antibody to NFATc2 in control and Orai1$^{-/-}$ T cells left unstimulated (naïve) or stimulated with anti-CD3 and anti-CD28 antibodies for 16 hours under T_H17-polarizing conditions. Data were normalized to the mean ChIP recovery of all experiments. **P<0.005, ***P<0.0005.

NIH-PA Author Manuscript
NIH-PA Author Manuscript
NIH-PA Author Manuscript

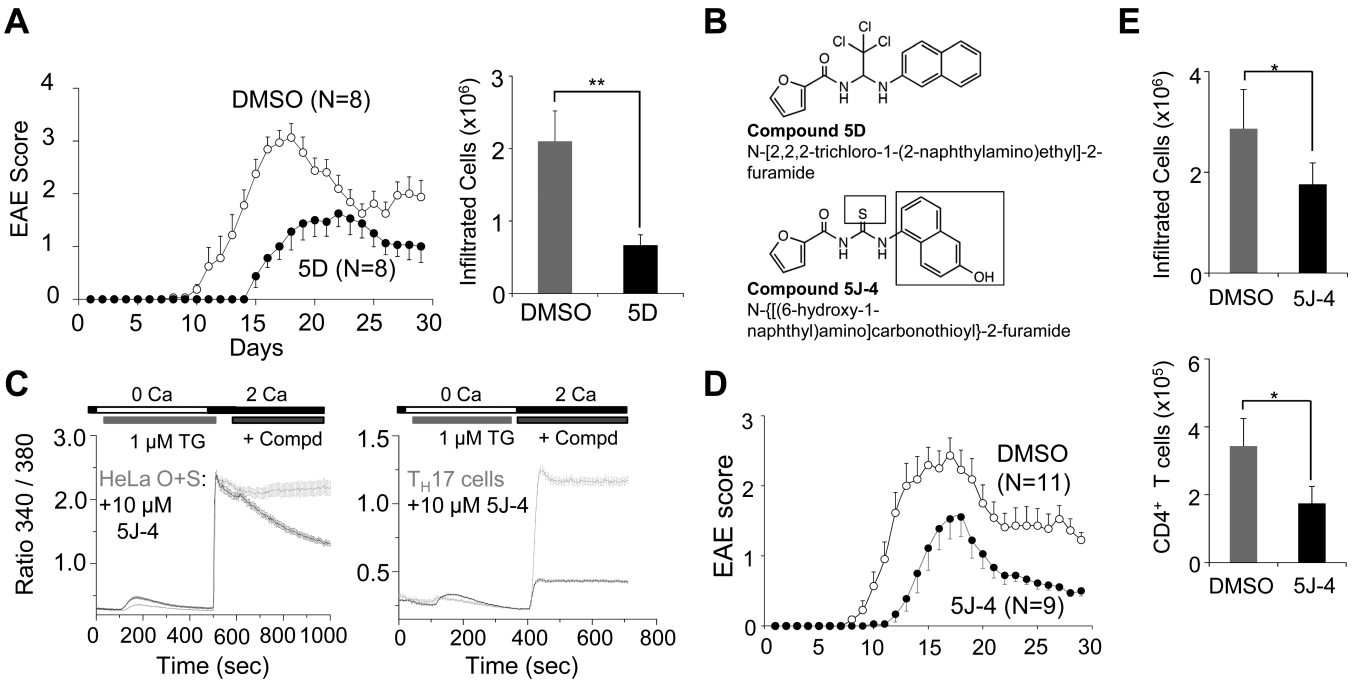

Figure 6. Compound 5D and 5J-4 ameliorate T_H17-mediated autoimmune disease

(**A**) EAE disease course in C57BL/6 mice injected intraperitoneally with either carrier alone or compound 5D (1 mg/kg) every alternate day starting from day −1. At day 0, disease was induced with injection of MOG_{35-55}/CFA. The graph shows average ± s.e.m. and is representative of three experiments with 8-10 animals in each experiment.

(**B**) Chemical structures of compound 5D and its analogue, compound 5J-4.

(**C**) Measurement of block of SOCE by compound 5J-4 in HeLa-OSN cells (left panel) or primary T_H17 cells (right panel). In all the graphs data represent average ± s.e.m. from 25-35 different cells.

(**D**) Compound 5J-4 ameliorates symptoms of experimental autoimmune encephalomyelitis (EAE) in vivo. EAE disease course in mice injected intraperitoneally with either DMSO or compound 5J-4 (2 mg/kg) every alternate day starting from day 0 after disease induction with MOG_{35-55}/CFA. The graph shows average ± s.e.m. from one of three independent repeats of the experiments with 10-20 mice per trial.

(**E**) Compound 5J-4 reduces infiltration of mononuclear cells into the CNS when administered in vivo. Mononuclear cells purified from the central nervous system of control and compound 5J-4-treated mice were counted (top) or examined for numbers of $CD4^+$ T cells (bottom) (n=4). *P<0.05, ***P<0.0005

NIH-PA Author Manuscript

NIH-PA Author Manuscript

NIH-PA Author Manuscript

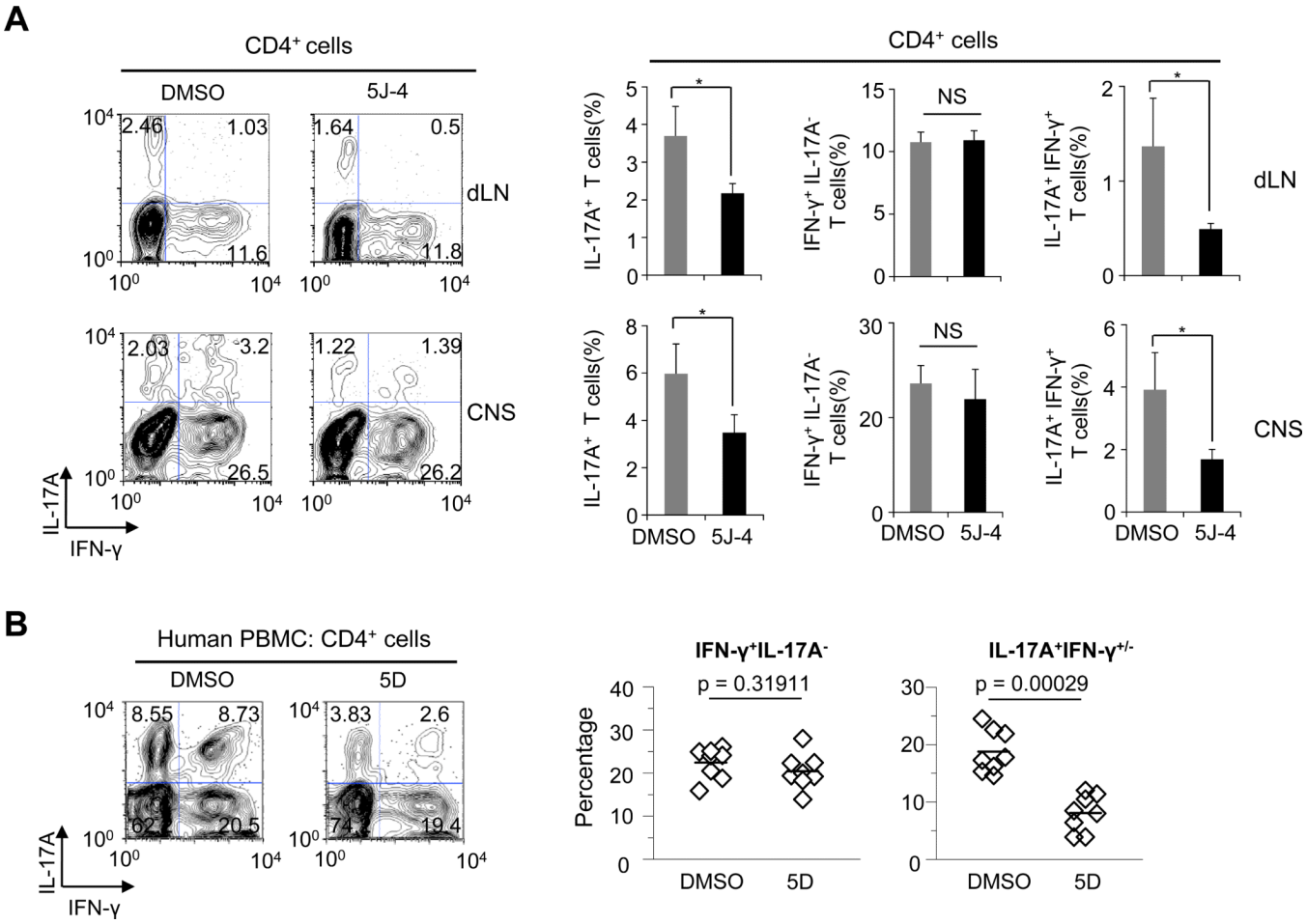

Figure 7. Treatment with CRAC channel blockers reduces differentiation and expansion of T_H17 cells

(**A**) Compound 5J-4 treatment preferentially decreases T_H17 differentiation in vivo. Expression levels of IFN-γ and IL-17A were measured in cells isolated from the draining lymph nodes (dLN) and CNS of DMSO and compound 5J-4-treated mice after 14 days of immunization with MOG_{35-55} peptide/CFA. Cells were stimulated with PMA and ionomycin and stained for CD4, IFN-γ, and IL-17A. Bar graphs on the right show average ± s.d.m. of indicated population of T cells from four mice.

(**B**) Suppression of expansion and maintenance of pre-differentiated human T_H17 cells by inhibition of CRAC channel activity. Human PBMCs were harvested, stimulated with anti-CD3 and anti-CD28 antibodies, and cultured with IL-1β and IL-23 in the presence of DMSO or 20 μM of compound 5D. Cells were restimulated with PMA and ionomycin at day 6 and examined for IL-17A and IFN-γ production. The graph shows results from eight donors.